GnRH-1 Neurons Are Not in the Goofy Group: 123cre Tracing Sets the Record Straight

Enrico Amato Jr.[1], Mia V. Call[1], Noah M. LeFever[1], Mya Aviles-Carlos[1], Nikki M. Dolphin[1], Paolo E. Forni[1]*

[1)] Department of Biological Sciences, The Center for Neuroscience Research, The RNA Institute, University at Albany, State University of New York, Albany, New York, USA.

*Corresponding author: pforni@albany.edu

Abstract

The olfactory placode (OP) gives rise to a wide array of chemosensory neurons in the nasal region, including olfactory sensory neurons, vomeronasal sensory neurons, and those of the septal organ and Grueneberg ganglion. During placodal invagination, the OP also produces migratory neurons such as gonadotropin-releasing hormone-1 (GnRH-1) neurons, terminal nerve (TN) neurons, and olfactory pioneer neurons, which are thought to initiate olfactory bulb development. Despite decades of research, the genetic lineage and molecular identity of OP-derived neuronal types remain under investigation. GnRH-1 neurons play essential roles in reproduction and chemodetection but appear genetically distinct from olfactory and vomeronasal chemosensory neurons. The Golgi-associated olfactory signaling regulator Goofy/Gfy is expressed in developing chemosensory neurons. To determine whether its expression is specific to nasal chemosensory epithelia or shared across OP derivatives, we characterized its expression and lineage at embryonic and postnatal stages. Our results confirm broad expression in developing chemosensory neurons and subsets of olfactory pioneer neurons, but not in GnRH-1 neurons, with only sparse expression in putative TN neurons. These findings reveal a previously unrecognized genetic distinction between nasal migratory and chemosensory neuronal populations.

Introduction

The olfactory placode (OP) is the ectodermal thickening responsible for the development of the olfactory system of vertebrates (Verwoerd and van Oostrom, 1979). In mice, the OP primordium can first be identified at E9.0 (embryonic day 9) (Ikeda et al., 2007; Klein and Graziadei, 1983; Rawson, 1999). The OP then invaginates around E10.5 (Brunjes and Frazier, 1986; Tarozzo et al., 1995) to give rise to the olfactory pit which further develops into multiple derivatives which include various specialized chemosensory epithelia: the main olfactory epithelium (OE), the vomeronasal organ (VNO), septal organ and Gruenberg ganglion (GG) (Couly and Le Douarin, 1985; Cuschieri and Bannister, 1975b). As the OP forms and then invaginates, it undergoes several waves of neurogenesis (Forni et al., 2013; Paronett et al., 2023; Rukh et al., 2024). Around E10.5, shortly after its formation, the OP is highly proliferative, and presents mitotic figures in the apical layers (Cuschieri and Bannister, 1975a; Graham et al., 2007; Smart, 1971; Taroc et al., 2020)

Between E10.5 and E11.5 the OP mostly produces migratory neurons that leave the OP and migrate toward the developing brain (Fornaro et al., 2003; Forni et al., 2011a; Murakami et al., 2022). The migratory neurons include the gonadotropin-releasing hormone-1 (GnRH-1) neurons, presumptive terminal nerve (TN), and the presumptive olfactory pioneer neurons, which are crucial for inducing olfactory bulb (OB) formation (Gong and Shipley, 1995). Around E11, the number of Achaete-scute homolog-1 (Ascl1)-expressing neuronal progenitors increases in the developing olfactory epithelia, and the neurogenesis of most chemosensory neurons is established (Guillemot et al., 1993; Taroc et al., 2020).

The GnRH-1 neurons are broadly accepted to have a placodal origin in vertebrates (Murakami et al., 2022; Schwanzel-Fukuda and Pfaff, 1989; Whitlock and Westerfield, 2000; Wray et al., 1989). The GnRH-1 neurons are ancestral cells (Herbison, 2025), in fact, both GnRH peptides and GnRH-expressing neurons have been reported in ascidians, where specialized olfactory chemosensory epithelia are absent and only proto-placodal

structures have also been described (Abitua et al., 2015; Kamiya et al., 2014; Poncelet and Shimeld, 2020; Sakai et al., 2020; Stolfi et al., 2015).

The TN neurons form the migratory mass, along with the olfactory pioneer neurons, neuropeptide-Y (Npy) expressing neurons, Somatostatin (Sst) expressing neurons, the GnRH-1 neurons, and the olfactory ensheathing cells (Demski and Schwanzel-Fukuda, 1987; Hilal et al., 1996; Miller et al., 2010; Murakami et al., 2022; Taroc et al., 2017; Valverde et al., 1993; Vilensky, 2012).

The migratory neurons emerging from the developing olfactory structures exhibit several molecular/genetic differences relative to the chemosensory neurons of the olfactory and vomeronasal epithelia. The GnRH-1 neurons express the transcription factor Isl1, which defines a unique genetic lineage across the neurons of the migratory mass (Lund et al., 2020; Shan et al., 2020; Taroc et al., 2020). Additionally, the GnRH-1 neurons can form in animals with loss-of-function mutations in the transcription factor Gli3, which instead causes severe impairment of olfactory and vomeronasal neurogenesis (Taroc et al., 2020). Furthermore, characterization of mice expressing the human Peripherin BAC transgene or Prokineticin Receptor 2-Cre (Prokr2Cre) suggests distinct genetic lineages between the migratory pioneer-TN neurons and the GnRH-1 neurons (Amato et al., 2024; Taroc et al., 2017).

GnRH-1, TN, and olfactory pioneer neurons are among the earliest neuronal populations to develop in the nose. Prokr2Cre lineage tracing showed that these cells can be identified genetically and through strong immunoreactivity for Cntn2 (TAG-1) and Map2 between E11.5 and E14.5. In contrast, little to no immunoreactivity for either marker is seen in the sensory neurons of the developing olfactory and vomeronasal epithelia (Amato et al., 2025; Schwarting et al., 2001; Taroc et al., 2017).

Patients affected by Kallmann syndrome are characterized by a defective sense of smell and delayed or absent puberty (Forni and Wray, 2015; Kallmann, 1944; Lieblich et al., 1982). Roles of GnRH-expressing neurons for chemodetection have been proposed from ascidians to vertebrates (Abitua et al., 2015; Umatani and Oka, 2019). Recent data have identified that a subpopulation of GnRH-1 neurons around the OB plays a role in processing

86 chemosensory signals (Decoster et al., 2024). Notably, this group of OB GnRH-1 neurons
87 has been shown to function in both mating behavior and in olfactory preference for
88 opposite-sex odors. These data indicate that GnRH-1 neurons, beyond their established
89 function in regulating the hypothalamic-pituitary-gonadal axis, can also play a crucial role
90 in processing chemosensory stimuli (Umatani and Oka, 2019).
91 The developmental relationship between the olfactory system and the other
92 neurons of the migratory mass has been a matter of investigation for decades. However,
93 the lack of distinct markers and defined genetic entry points has hindered efforts to identify
94 early nasal neurons and clarify the functions of specific genes in their development. The
95 Golgi Associated Olfactory Signaling Regulator (Goofy/ Gfy) is an integral membrane
96 protein located in the Golgi membrane, which is expressed in nasal chemosensory neurons
97 of rodents, including neurons of the main olfactory epithelium (OE), vomeronasal sensory
98 epithelium (VSE), and GG (Kaneko-Goto et al., 2013). Here, we characterized Gfy
99 expression and genetic lineage during early stages of olfactory development (E11.5-E15.5)
100 and the postnatal VNO. Our data indicates a molecular distinction and differences in
101 developmental dynamics between the migratory neuronal population originating from the
102 OP and the neurons belonging to the specialized chemosensory system of rodents.
103
104 **Results**
105
106 **Gfy is heterogeneously expressed across newly formed neurons in the developing**
107 **olfactory system**
108 The developing OP and its derivatives are highly neurogenic, resulting in continuous
109 and asynchronous neuronal production throughout the nasal region. In mouse,
110 neurogenesis in the OP starts soon after its formation around E9.5, as pioneer neurons can
111 be already detected at E10.5 (Chen et al., 2009; Fornaro et al., 2003; Forni et al., 2011b;
112 Katoh et al., 2011). Analyzing single-cell RNA sequencing data of the nasal area at E14.5
113 (Fig. 1A) (Amato et al., 2024), we found Gfy expression in cell clusters containing the
114 olfactory maturation marker gene Omp (Olfactory marker protein) expressing putative

115 developing chemosensory neurons (OSNs/VSNs), as well as in some of the putative
116 migratory pioneer/TN neurons (positive for Prokr2) (Amato et al., 2024) (Fig. 1F,H,I). By
117 analyzing Gfy expression (Fig. 1A-I) and its correlation (Fig. 1J) with markers of
118 neurogenesis and olfactory maturation, we found that Gfy is not expressed by proliferative
119 olfactory-vomeronasal progenitors (Ascl1+) (Fig. 1B), nor by olfactory-vomeronasal
120 precursors expressing Neurod1 and Neurog1 (Fig. 1C-D). However, its expression
121 correlates with the RNA binding protein Elav3 (HuC) (Fig. 1E) and reaches its highest
122 correlation with Gap43 (Growth Associated Protein 43), a neuron-specific protein
123 expressed during axon growth (Karns et al., 1987; Verhaagen et al., 1989) (Fig. 1G, J). Gfy
124 expression is further retained in cells expressing mRNA of Omp (Fig. 1G-J). These data
125 support Gfy expression across various postmitotic maturing neurons originating from the
126 OP (Kaneko-Goto et al., 2013; Margolis, 1972; Margolis and Tarnoff, 1973).
127
128 **The GfyCre (123Cre) mouse line can produce different recombination patterns; in**
129 **chemosensory epithelia recombination starts to be apparent at E12**
130 To further characterize the Gfy genetic lineage across the various neurons
131 originating from the OP, we bred GfyCre mice with homozygous R26tdTomato (Ai14$^{-/-}$)
132 reporter mice. PCR analysis of the pups showed Cre inheritance following the expected
133 Mendelian ratios (data not shown); however (Fig. S1A-C), among the Cre-positive pups, we
134 observed two recombination patterns: 1) a highly chimeric recombination throughout the
135 body, including the chemosensory epithelia, and 2) recombination limited to the
136 chemosensory regions of the developing nose. Notably, similar recombination patterns
137 were seen regardless of whether the Cre was inherited maternally or paternally. From this
138 point on, we will discuss only results from animals in which recombination is limited to the
139 nasal chemosensory epithelia.
140 We examined embryos at multiple stages from E11.5 to E15.5 (Fig. 2). At E11.5, only
141 a few neurons positive for recombination were observed, some of which appeared in the
142 developing OE and VNO, whereas others were seen in the nasal mesenchyme (Fig. 2A). At
143 E12.5 and E13.5, neurons positive for recombination were clearly detected in the

144 developing chemosensory epithelia and in migratory neurons associated with Peripherin-
145 positive fibers (Fig. 2B-C). By E14.5 and E15.5, widespread recombination was evident
146 across the olfactory-vomeronasal epithelia and their projections to the OB (Fig. 2D-E), as
147 well as in neurons of the Gruenberg ganglion (GG) (Fig. S2) (Kaneko-Goto et al., 2013).
148 Notably, at these stages, we also observed Peripherin-positive fibers resembling those of
149 the putative TN invading the brain ventrally to the OB, which appeared negative for
150 recombination (Fig. 2D-E)(Fueshko and Wray, 1994; Wray et al., 1994). The migratory
151 neurons forming within the OP are readily detectable at E10.5 (Fornaro et al., 2003; Forni et
152 al., 2011b; Miller et al., 2010), prior to the initial neurogenesis of the olfactory/vomeronasal
153 chemosensory neurons that begins around E11.5 (Rawson et al., 2010; Taroc et al., 2020).
154 Around 2-3 days after the beginning of neurogenesis in the OP (E11.5 and E12.5), the
155 vomeronasal epithelium and part of the migratory mass showed only sparse GfyCre
156 recombination(Fig. 2A-B).
157 To better determine the time reference between the birth of chemosensory neurons
158 and GfyCre recombination, we injected GfyCre$^{+/-}$/A14$^{-/-}$ embryos with EdU first at E10.5,
159 then again at E11.5, and analyzed them at E14.5. (Fig. 3A). At this stage, we found that only
160 ~60% (SD ± 3.02) of EdU-positive neurons born 3 or 4 days before showed detectable
161 recombination (Fig. 3B-E). Altogether, this indicates that GfyCre-mediated recombination
162 is variably detected between 2 and 4 days after neurogenesis.
163
164 **Gfy is neither expressed by the GnRH-1 neurons nor by other neurons migrating from**
165 **the nose to the brain.**
166 After confirming that GfyCre mice exhibited the expected recombination in
167 chemosensory neurons within 3 days from neurogenesis, we aimed to understand if the
168 Gfy lineage included ancestral cells such as the TN neurons, GnRH-1 neurons, or other
169 neuronal populations that form in the nose and migrate to the brain (Hilal et al., 1996;
170 Murakami et al., 2022; Murakami et al., 2024). The GnRH-1 neurons form between E10 and
171 E12 (Jasoni et al., 2009; Schwanzel-Fukuda and Pfaff, 1989; Wray et al., 1989). To trace
172 different neurogenic waves of the GnRH-1 neurons in GfyCre/Ai14 embryos, some dams

173 were injected with EdU at E8.5 and E9.5, and others at E10.5 and E11.5 (Fig. S3). We found
174 that 15% (SD ± 5.35) of the GnRH-1 neurons were labeled by EdU injection at E8.5 and E9.5
175 (Fig. S3B-C''), while 40% (SD ± 7.59) were labeled after injections at E10.5 and E11.5 (Fig.
176 S3D-F''). Notably, at all analyzed stages (E11.5 to E15.5) we never found GnRH-1 neurons
177 or other neuronal cells positive for Gfy tracing in the brain (Fig. 4), suggesting that Gfy is not
178 expressed in newly formed or maturing GnRH-1 neurons even 6 days after neurogenesis.
179 However, EdU injections at E10.5 and E11.5 revealed that 50% (SD ± 2.97) of migratory Gfy
180 traced neurons in the nose were labelled with EdU at these stages (Fig. S4) (Change images
181 for Fig. S4).
182
183 **The terminal nerve neurons are negative for GfyCre tracing**
184 In a recent paper, Prokr2 was identified as a reliable genetic marker for the neurons
185 forming the TN as well as for putative olfactory pioneer neurons. In the developing nose,
186 migratory cells positive for Prokr2Cre/Ai14 tracing can also be identified based on high
187 immunoreactivity for Map2 up to E14.5 (Amato et al., 2024). However, by pairing GfyCre
188 tracing with Map2 immunostaining at E14.5, we found that only a subset of Map2-positive
189 migratory neurons were also positive for GfyCre tracing (Fig. 5A-B'').
190 In line with work done in chick (Murakami et al., 2022), we observed that also in mouse,
191 cells expressing Sst emerge from the developing VNO and appear to migrate as part of the
192 migratory mass toward the brain, however, Sst expressing cells were not positive for Gfy
193 tracing (Fig. 5C-E). In contrast, by using Prokr2Cre tracing, we observed that Sst is
194 expressed at least transiently by some of the Prokr2 traced migratory cells (Fig. 5F-H''). In
195 Prokr2 traced animals immunolabelled against Sst, we found that some of the Sst
196 expressing cells, were also positive for Prokr2 tracing in the migratory mass. However, Sst
197 expressing cells in the brain appeared to be negative for both GfyCre and Prokr2Cre tracing.
198 (Fig. 5H-H'').
199 Analyzing GnRH-1 migration (Fig. 4D), we could see that the GnRH-1 neurons
200 invading the brain, were not associated with GfyCre traced fibers. In fact, the Peripherin+

fibers of the TN appeared negative for Gfy tracing (Fig. 2), though sparse axons positive for Gfy tracing could be found in the basal forebrain (Fig. S5B-B’’).

To determine whether Gfy-tracing could discriminate among different subpopulations of Map2–Prokr2–expressing migratory neurons, we compared E14.5 GfyCre and Prokr2Cre lineage-traced embryos (Fig.5I-I’’). In Prokr2Cre-traced animals, neuronal cell bodies and fibers extended into the brain alongside the migrating GnRH-1 neurons. In contrast, GfyCre tracing labeled only neurons that remained within the nasal region. No GfyCre traced cell bodies enter the forebrain (Fig. 2, 4). These results suggest that while the migratory neurons expressing Prokr2, GnRH-1, and Sst invade the brain, the cell bodies belonging to the GfyCre lineage remain in the nose.

Following Gfy expression in postnatal VSNs revealed differences in the developmental dynamics of V1R and V2R VSNs.

The expression of Gfy in newly generated neurons makes this line a valuable tool for manipulating chemosensory neurons prior to their maturation. Because of our focus on neuronal populations of and arising from the vomeronasal primordium, we further examined Gfy expression in this area. During embryonic development, we found that GfyCre recombined in both Meis2 and AP-2ε (Tfap2e) expressing neurons, which later will mature into V1R and V2R VSNs respectively (Fig. S6) (Enomoto et al., 2011; Katreddi et al., 2022).

To characterize GfyCre recombination in relation to postnatal vomeronasal neurogenesis, we reanalyzed whole-VNO single cell RNA-sequencing datasets (Hills et al., 2024; LeFever et al., 2024) and reconstructed the canonical dichotomy of apical and basal VSN development (Fig. 6A). UMAP projections and expression overlays for progenitors (Ascl1, Mki67, Neurog1), precursors (non-proliferative Neurog1, Neurod1), maturing VSNs (Gap43, Gng8/Gy8 and Gfy) and the maturation marker Omp. These recapitulated the expected neurogenic sequence, with progenitors at the base of the Y-trajectory, transitioning through neuronal precursors and immature VSNs, and diverging into the

230 apical and basal branches, which culminate in mature V1R/Meis2+ and V2R/AP-2ε+
231 neurons (Fig. 6B).
232 Pearson coefficient calculation of global gene–gene correlation revealed consistent
233 transcriptional changes across the dataset (Fig. 6C). This analysis showed that in contrast
234 to what was observed during embryonic development (Fig. 1J), a negative correlation
235 between Gfy and Gap43, along with a positive correlation between Gng8 and Omp. This
236 suggests that postnatally, Gfy is expressed with a delay relative to Gap43 in maturing
237 neurons and maintains high expression in mature neurons, while Gng8 clusters with
238 intermediate neuronal states (Fig. 6D,G).
239 When the apical and basal branches were examined separately, we found additional
240 interesting differences in their internal development (Fig. 6E–E"). In fact, we noticed that
241 Gap43 expression rises earlier in Meis2+/apical lineage as opposed to AP-2ε+/basal
242 lineage (Fig. 6E', E''). On the contrary, the Meis2-/basal lineage was found to have a
243 negative correlation between Neurod1 and Gap43.
244 Further analysis at precursor stages reinforced this difference (Fig. S7), showing
245 higher Gap43 and Gfy expression in the Meis2+/apical lineage. Moreover, by performing
246 correlation analysis on Meis2+/apical and AP-2ε+/basal precursor populations, we
247 observed that Meis2+ cells have a more precocious expression of Gfy, partial overlapping
248 with Neurod1 and Omp (Fig. S7C'-C''). Suggestive of differences in developmental
249 dynamics between the two main types of VSNs.
250 From previous work we know that V2R VSN specific transcription factor Ap2e
251 directly binds and negatively regulates the expression of the Gt(ROSA)26Sor locus (Lin et
252 al., 2022). Based on that, we assessed expression of the Gt(ROSA)26Sor locus to evaluate
253 baseline reporter activity across VSN classes. Violin plots revealed a modest but
254 consistent elevation in ROSA expression in apical (Meis2+) VSNs relative to basal neurons
255 (AP-2ε+) (Fig. 6F), suggesting lineage-specific differences that may influence reporter
256 sensitivity in genetic tracing experiments.
257

258 To validate some of these observations in vivo, we combined GfyCre lineage tracing with
259 Gap43 immunofluorescence (Fig. 7A-A'''). At P30, GfyCre-traced neurons were present in
260 both immature and mature VSNs. However, a difference in the intensity of tdTomato
261 expression was visibly noticeable between neurons in the apical and basal territories (Fig
262 7A-A"). In the marginal zones, where the VSNs give rise to maturing Gap43+ cells, we
263 noticed that tdTomato fluorescence was often absent or very low, confirming that GfyCre-
264 mediated recombination lags behind Gap43 expression.
265 As expected from their known axonal guidance programs, V1R/Meis2+ VSNs (Neuropilin-
266 2+) projected to the anterior AOB, whereas V2R/AP-2ε+ VSNs (Robo2+) projected to the
267 posterior AOB. GfyCre-mediated recombination was detected in the axons targeting both
268 AOB domains (Fig. 7B-B''). The reduced Rosa26 expression characteristic of basal VSNs
269 again translated into visibly weaker tdTomato signals in the posterior AOB glomeruli
270 compared to those in the anterior AOB glomeruli (Fig. 6F).
271
272 **Discussion**
273 The lineage and developmental relationship between olfactory sensory neurons
274 (OSNs) and neurons of the migratory mass in the developing nose has been a subject of
275 much speculation. Early observations showed that the GnRH-1 neurons emerge from the
276 OP and migrate alongside olfactory axons toward the forebrain, suggesting that a caudal
277 branch of the vomeronasal nerve might provide structural or molecular cues essential for
278 GnRH-1 pathfinding to the basal forebrain (Hanchate et al., 2012; Schwanzel-Fukuda and
279 Pfaff, 1989; Wierman et al., 2011; Wray et al., 1989). This idea was strengthened by findings
280 in Kallmann syndrome (Kallmann, 1944), where anosmia frequently co-occurs with failed
281 GnRH-1 neuronal migration, implying a shared developmental dependency (Schwarting et
282 al., 2001; Yoshida et al., 1995). However, subsequent work has suggested that the
283 association between OSNs and GnRH-1 neurons is less direct than initially assumed.
284 Accumulating evidence indicates that populations of neurons distinct from OSNs and
285 VSNs serve as the primary substrates guiding GnRH-1 neurons into the brain (Amato et al.,
286 2025; Amato et al., 2024; Murakami et al., 2024; Taroc et al., 2019; Taroc et al., 2020; Taroc

287 et al., 2017). This evolving understanding has shifted the field away from the long-held
288 assumption of a direct OSN/VSN-GnRH link and toward a model in which multiple
289 placode-derived neuronal lineages play specialized and non-redundant roles in GnRH-1
290 migration (Murakami et al., 2022).
291 Here, we present a characterization of the neuronal cell types within the developing
292 olfactory system that can be genetically traced through the use of Gfy(123)Cre.
293 Characterizing the mice, we observed that 50% of the Cre-positive mice exhibit some early
294 Gfy expression during development that can lead to chimeric recombination (Fig. S1). This
295 is an important caveat for designing genetic strategies with this line, we suggest keeping
296 these mice on a reporter line to monitor the recombination pattern. However, at least 50%
297 of the GfyCre mice have the expected olfactory recombination.
298 From the experiments shown here, we provide new evidence distinguishing GnRH-1
299 neurons and other TN neuron cells from the OSN, VSN and GG lineages. Initial analysis of
300 Gfy expression using E14.5 single-cell RNA sequencing data revealed that both
301 differentiated olfactory neurons and groups of migratory neurons in the nose exhibit Gfy
302 enrichment (Fig. 1). Moreover, these data showed that Gfy largely overlaps with Gap43
303 expression during embryonic development (Fig. 1J). Consistent with these transcriptomic
304 findings, examination of GfyCre$^{+/-}$;Ai14$^{+/-}$ traced embryos revealed a progressive increase in
305 Gfy lineage tracing between E11.0 and E15.5, spanning many OSNs, VSNs, and GG
306 neurons, as well as their projections to the developing OBs (Fig. 2, S2). In addition, we also
307 identified subsets of Gfy labeled cell bodies that appeared to be migrating away from the
308 chemosensory epithelia toward the developing OBs (Fig. 2B-C). These results indicate that
309 some of the migratory neurons express Gfy, supporting prior observations that Gfy
310 expression is associated with neuronal populations forming from or belonging to the nasal
311 chemosensory epithelia (Baker and Farbman, 1993; Habif et al., 2023; Hirata et al., 2006;
312 Kaneko-Goto et al., 2013; Valverde et al., 1993).
313
314 Recent work identified Sst expression in cells invading the brain with the GnRH-1
315 neurons (Murakami et al., 2022). We observed that Sst is expressed by some of the

316 Prokr2Cre traced neurons but not positive for GfyCre tracing (Fig. 5C-H’’).However, recent
317 data in mouse suggests that the GnRH-1 neurons themselves can express Sst, making it
318 possible that previously identified Sst cells include subsets or maturing GnRH-1 neurons
319 (Zouaghi et al., 2025). No overlap between GnRH-1, Sst, and Gfy tracing was observed at
320 any point during the development or migration of the GnRH-1 neurons (Fig. 4,5).
321 Interestingly, GnRH-1 immunoreactivity appears days before the onset of GfyCre
322 recombination. In fact, while at E11.5 and E12.5, numerous neurons within the VNO and
323 nasal area were positive for GnRH-1, only sparse cells showed detectable Gfy lineage
324 tracing (Fig. 4A-B’’’).
325 Our birth-dating experiments indicate that chemosensory neurons in the OE and
326 VNO undergo Cre-mediated recombination between 3-4 days after neurogenesis (Fig. 3).
327 Birth dating of GnRH-1 neurons confirmed that GfyCre recombination is not detectable in
328 these cells even 6 days after their generation (Fig. S3).
329 We previously identified that Prokr2Cre tracing and Map2 strong immunoreactivity
330 overlap in migratory TN neurons emerging from the developing olfactory epithelia. Notably,
331 some Prokr2+ expressing neurons also express GnRH-1 (Amato et al., 2024).
332 Map2 immunostaining combined with GfyCre lineage tracing revealed that approximately
333 50% of the migratory neurons within the migratory mass were positive for Gfy tracing (Fig.
334 5A–D). These findings indicate that at least half of the neurons previously identified by
335 Prokr2 lineage tracing also express Gfy, consistent with the embryonic single-cell
336 transcriptomic data (Fig. 1). Together, these data suggest that Prokr2 exhibits broader
337 expression across migratory neuronal populations, including olfactory pioneer and TN
338 neurons, while GfyCre is limited only to pioneer neurons that remain in the nasal
339 compartment. The GnRH-1 neurons enter the brain along TN fibers, which are positive for
340 Cntn2 (Tag1), Peripherin and Prokr2Cre lineage (Amato et al., 2025; Schwarting et al., 2001;
341 Taroc et al., 2017). However, Peripherin-positive TN projections that invade the basal
342 forebrain together with the GnRH-1 neurons were for the most part negative for Gfy tracing
343 (Fig. 2, S5). GfyCre does not label the GnRH-1 neurons, nor other cell bodies that invade
344 the brain.

Following Gfy expression and recombination in the VNO lead us to some other interesting findings. GfyCre recombination occurs in neurons of both apical (Meis2/V1R) and basal (AP-2ε/V2R) vomeronasal lineages, indicating that Gfy is not lineage-restricted (Fig. 6). However, reanalysis of postnatal single-cell transcriptomic data of apical and basal trajectories reveals subtle but important differences in their maturation dynamics. Apical VSNs display earlier and stronger overlap between Gap43 and Gfy expression, whereas basal VSNs show delayed or weaker expression suggesting lineage-specific developmental gene expression progressions (Fig. 6E-E'') (Hills et al., 2024; Lin et al., 2018). These intrinsic differences extend to reporter sensitivity at the Rosa26 locus (Fig. 6F), which exhibits lower baseline expression in basal VSNs (Lin et al., 2022) and likely contributes to weaker lineage-tracing signals in this population (Fig. 6F).

In vivo validation confirmed that GfyCre recombination lags behind early differentiation markers such as Gap43, yet robustly labels neurons as they progress toward maturity and project appropriately to both anterior and posterior domains of the accessory olfactory bulb. Together, these findings establish Gfy as a developmentally timed marker of postmitotic vomeronasal neurons, refine the interpretation of Cre-based lineage tracing across VSN subtypes, and provide a framework for selectively manipulating chemosensory neurons without perturbing earlier neurogenic events.

374
375
376
377
378
379
380 **Methods**

381 **Animals**

382 Gfy(123)-Cre mice were provided generously from Dr. Thomas Bozza (Northwestern
383 University), originally generated at RIKEN Brain Science Institute, Japan (Dr. Yoshihiro
384 Yoshihara). PCR analysis was performed for genotyping, using generic Cre primers as
385 follows: Cre FWD, AGG TGT AGA GAA GGC ACT TAG C, *Cre RVS, CTA ATC GCC ATC TTC*
386 *CAG CAG G*. Ai14 mice were genotyped following the B6.Cg-*Gt(ROSA)26Sor*$^{tm14(CAG-}$
387 $^{tdTomato)Hze}$/J protocols available on jax.org. Generation of Prokr2Cre$^{+/-}$ mice (Mohsen et al. 2017)
388 and genotyping (Amato Jr. et al. 2024) were previously described. CO_2 euthanasia was
389 performed, then immediate cervical dislocation. Mice of either sex were used for
390 experiments. All animal experiments and procedures were completed in accordance with
391 the guidelines of the Animal Care and Use Committee at the University at Albany, SUNY.
392
393 **Tissue Preparation**

394 **Embryonic Tissue Collection**

395 Embryo collection was carefully performed on time-mated females, where observation of
396 the vaginal plug was estimated to be embryonic day 0.5 (E0.5). Collected embryos were
397 placed into 3.7% formaldehyde/PBS at 4°C for 2 h to fix. Embryos then were submerged in
398 30% sucrose overnight, then embedded and frozen in O.C.T (Tissue-Tek) before storing at
399 −80°C. The CM3050S Leica cryostat was used to cryosection embedded embryos, tissue
400 sections were collected using Superfrost plus slides (VWR) at 18 µm thickness for
401 immunofluorescent staining.
402

403 **Postnatal Tissue Collection**

404 P30 mice were sedated with Sodium Pentobarbital, then transcardial perfusion was
405 performed with 1X PBS followed by 4% Paraformaldehyde in PBS. Noses were separated
406 from brains, with the noses being post fixed in 4% Paraformaldehyde overnight at 4°C.
407 Brains were post fixed in 1% Paraformaldehyde overnight at 4°C. The following day, brains
408 were cryoprotected with 30% Sucrose in 1X PBS at 4°C overnight and noses were incubated
409 in 500mM EDTA in 1X PBS for decalcification. At end of EDTA incubation noses were
410 cryoprotected in sucrose. Samples were embedded and frozen in O.C.T and stored in -80°C
411 prior to cryosectioning serial sections on Superfrost plus (VWR) slides. Noses were
412 sectioned in a coronal orientation, while brains were sectioned in the parasagittal
413 orientation.

414

415 **Immunohistochemistry**

416 The following primary antibodies and dilutions were used for this study: goat-α-RFP
417 (1:1000, Rockland), chicken-α-Peripherin (1:500, Abcam), SW rabbit-α-GnRH-1 (1:6000,
418 Susan Wray, NIH), rabbit-α-Map2 (1:150, Cell Signaling Technology), mouse-α-RFP (1:500,
419 Origene), rabbit-α-Somatostatin (1:100, Abcam), rabbit-α-Gap43 (1:1000, Abcam), goat-α
420 Neuropilin2 (1:4000, R&D Systems), mouse-α-Robo2 (1:50, Santa Cruz), rabbit-α-RFP
421 (1:500, Rockland), goat-α-OMP (1:4000, WAKO), goat-α-AP-2ε (1:500, R&D Systems), and
422 rabbit-α-Meis2 (1:1000, Abcam).
423 Antigen retrieval was used for experiments utilizing rabbit-α-Map2, mouse-α-RFP, goat-α
424 Neuropilin2, mouse-α-Robo2, rabbit-α-RFP, goat-α-AP-2ε, and rabbit-α-Meis2, slides were
425 submerged in a citric acid solution, gradually heated to 95°C, once at 95°C, boiling for
426 15 min. Slides were then cooled for 15 min before proceeding with standard
427 immunohistochemical protocol.

428

429 **Immunofluorescence**

430 For immunofluorescent staining, secondary antibodies selected for the correct species
431 were conjugated with Alexa Fluor-488, Alexa Flour-594, or Alexa Flour-680 (Invitrogen and

432 Jackson Laboratories). 4',6'-diamidino-2-phenylindole (DAPI, 1:3000; Sigma-Aldrich) was
433 used to counterstain sections and coverslips were mounted using Fluorogel l (Electron
434 Microscopy Sciences). Confocal microscopy image acquisition was taken on a LSM 710
435 microscope (Zeiss). Epifluorescence images were acquired on a DM4000 B LED
436 fluorescence microscope equipped with a Leica DFC310 FX camera. Whole embryo
437 images were acquired using the Nikon SMZ25 stereo microscope. Image analysis and
438 quantifications were done using FIJI/ImageJ software. Each staining presented was
439 replicated on three different animals.
440
441 **Edu Administration and Detection**
442 Edu was prepared according to ClickTech EdU Cell Proliferation Kit 488 for IM (Millipore-sigma,
443 BCK-EDU488). Edu injections were performed on time-mated females previously described in
444 the tissue preparation section of the methods. Intraperitoneal injections were done at various
445 time points at a dosage of 50mg/kg body weight. We observed that development was not affected
446 by the injections. To detect Edu positive cells, we performed immunofluorescence as described in
447 the previous section and followed the standard ClickTech EdU Cell Proliferation Kit 488 protocol.
448 Slides were incubated for 30 minutes at room temperature in the prepared detection solution
449 protected from light. After, we followed standard immunofluorescent protocol.
450
451
452 **Cell Quantifications**
453 Quantifications performed were done in FIJI/ImageJ using the cell counter plugin. All cell
454 number quantifications in the nasal region were done on parasaggital E12.0-P1 tissue. For
455 each quantification reported, cell bodies of neurons were counted. For all quantifications
456 of cell counts, the number of cells per section (~5 sections) was averaged for each animal.
457
458
459 **Embryonic Single-Cell Cell RNA Sequencing**

460 Dimplots and feature plots were generated in R studio using the Seurat R package. The
461 E14.5 single-cell sequencing data can be found on the Gene Expression Omnibus (GEO)
462 database: GEO accession number GSE234871
463 (**https://www.ncbi.nlm.nih.gov/geo/query/acc.cgi?acc=GSE234871**). The data
464 collection process and analysis was previously described (Amato Jr. et al. **2024**).
465 **Post-natal scRNA-seq quality control, clustering and analysis.**
466 Quality Control and Filtering: Postnatal single-cell RNA sequencing datasets (P14, P56, and
467 P10, P21, P60) used for analysis can be found with GEO accession numbers GSE247872,
468 and GSE252365. Data collection and analysis were previously described (Hills et al., 2024;
469 LeFever et al., 2024). Independent ages respective datasets were merged and integrated to
470 get a more full picture of the vomeronasal development. Cell filtering was done
471 downstream to remove genes expressed in ≤3 cells, and ≥200 detectable genes. Quality
472 control was done to clean up the data to only cells expressing between 200 and 9000 with
473 ≤25% of those genes being mitochondrial genes.
474 CellCycle Regression: To avoid noise from cells undergoing active cell cycling, cells were
475 scored for their features aligning with S, and G2/M phase as described in a SeuratV5
476 vignette (Hao et al., 2023). The difference between S.Score and G2M.Score was calculated,
477 and these cells were regressed to include differences between cell types but remove
478 differences within cycling cells.
479 DoubletFinder: The DoubletFinder program built for Seurat was applied to reduce and
480 remove a predicted number of artificial doublets created during the process of single cell
481 sequencing. This package was used as previously described (McGinnis et al., 2019).
482 Processing: Using SCTransform the data was scaled and normalized, the top 2000 highly
483 variable features within the top 50 principal components were used for clustering. About
484 18,000 cells were used in this analysis and different developmental stages were identified
485 through well documented key markers. When completing analysis each cluster/gene were
486 compared against all other clusters/genes. In the Apical/V1R v Basal/V2R comparisons,
487 only the Apical/V1R lineage was compared to the Basal/V2R lineage. Analysis of the

differential Gt(ROSA)26Sor expression was conducted on P10, P21, P60 data previously published (LeFever et al., 2024).

Acknowledgements

This work was supported by the Eunice Kennedy Shriver National Institute of Child Health and Human Development (NICHD) under Grants R01HD09733 (P.E.F.) and R01HD114827 (P.E.F.), as well as by the National Institute on Deafness and Other Communication Disorders (NIDCD) under Grant R01DC017149 (P.E.F.). The Zeiss 980 microscope at the University at Albany was funded by the Office of the Director, NIH, under Award Number S10OD028600.

We thank Dr. Yoshiro Yoshihara (Riken Center for Brain Science, Japan) and Dr. Thomas Bozza (Department of Neurobiology, Northwestern University, USA) for donating and sharing the Gfy Cre line with us.

References

Abitua, P. B., Gainous, T. B., Kaczmarczyk, A. N., Winchell, C. J., Hudson, C., Kamata, K., Nakagawa, M., Tsuda, M., Kusakabe, T. G. and Levine, M. (2015). The pre-vertebrate origins of neurogenic placodes. *Nature* **524**, 462-465.

Amato, E., Jr., Semon, A. M. and Forni, P. E. (2025). Tracing Early Migratory Neurons in the Developing Nose Using Contactin-2 (Cntn2) CreERT2. *Genesis* **63**, e70021.

Amato, E., Jr., Taroc, E. Z. M. and Forni, P. E. (2024). Illuminating the terminal nerve: Uncovering the link between GnRH-1 neuron and olfactory development. *J Comp Neurol* **532**, e25599.

Baker, H. and Farbman, A. I. (1993). Olfactory afferent regulation of the dopamine phenotype in the fetal rat olfactory system. *Neuroscience* **52**, 115-134.

Brunjes, P. C. and Frazier, L. L. (1986). Maturation and plasticity in the olfactory system of vertebrates. *Brain Res* **396**, 1-45.

Chen, B., Kim, E. H. and Xu, P. X. (2009). Initiation of olfactory placode development and neurogenesis is blocked in mice lacking both Six1 and Six4. *Dev Biol* **326**, 75-85.

Couly, G. F. and Le Douarin, N. M. (1985). Mapping of the early neural primordium in quail-chick chimeras. I. Developmental relationships between placodes, facial ectoderm, and prosencephalon. *Dev Biol* **110**, 422-439.

Cuschieri, A. and Bannister, L. H. (1975a). The development of the olfactory mucosa in the mouse: electron microscopy. *J Anat* **119**, 471-498.

---- (1975b). The development of the olfactory mucosa in the mouse: light microscopy. *J Anat* **119**, 277-286.

Decoster, L., Trova, S., Zucca, S., Bulk, J., Gouveia, A., Ternier, G., Lhomme, T., Legrand, A., Gallet, S., Boehm, U., et al. (2024). A GnRH neuronal population in the olfactory bulb translates socially relevant odors into reproductive behavior in male mice. *Nat Neurosci* **27**, 1758-1773.

Demski, L. S. and Schwanzel-Fukuda, M. (1987). The terminal nerve (nervus terminalis): structure, function, and evolution. Introduction. *Ann N Y Acad Sci* **519**, ix-xi.

Enomoto, T., Ohmoto, M., Iwata, T., Uno, A., Saitou, M., Yamaguchi, T., Kominami, R., Matsumoto, I. and Hirota, J. (2011). Bcl11b/Ctip2 controls the differentiation of vomeronasal sensory neurons in mice. *J Neurosci* **31**, 10159-10173.

Fornaro, M., Geuna, S., Fasolo, A. and Giacobini-Robecchi, M. G. (2003). HuC/D confocal imaging points to olfactory migratory cells as the first cell population that expresses a post-mitotic neuronal phenotype in the chick embryo. *Neuroscience* **122**, 123-128.

Forni, P. E., Bharti, K., Flannery, E. M., Shimogori, T. and Wray, S. (2013). The indirect role of fibroblast growth factor-8 in defining neurogenic niches of the olfactory/GnRH systems. *J Neurosci* **33**, 19620-19634.

Forni, P. E., Fornaro, M., Guenette, S. and Wray, S. (2011a). A role for FE65 in controlling GnRH-1 neurogenesis. *J Neurosci* **31**, 480-491.

Forni, P. E., Taylor-Burds, C., Melvin, V. S., Williams, T. and Wray, S. (2011b). Neural crest and ectodermal cells intermix in the nasal placode to give rise to GnRH-1 neurons, sensory neurons, and olfactory ensheathing cells. *J Neurosci* **31**, 6915-6927.

Forni, P. E. and Wray, S. (2015). GnRH, anosmia and hypogonadotropic hypogonadism--where are we? *Front Neuroendocrinol* **36**, 165-177.

Fueshko, S. and Wray, S. (1994). LHRH cells migrate on peripherin fibers in embryonic olfactory explant cultures: an in vitro model for neurophilic neuronal migration. *Dev Biol* **166**, 331-348.

Gong, Q. and Shipley, M. T. (1995). Evidence that pioneer olfactory axons regulate telencephalon cell cycle kinetics to induce the formation of the olfactory bulb. *Neuron* **14**, 91-101.

Graham, A., Blentic, A., Duque, S. and Begbie, J. (2007). Delamination of cells from neurogenic placodes does not involve an epithelial-to-mesenchymal transition. *Development* **134**, 4141-4145.

Guillemot, F., Lo, L. C., Johnson, J. E., Auerbach, A., Anderson, D. J. and Joyner, A. L. (1993). Mammalian achaete-scute homolog 1 is required for the early development of olfactory and autonomic neurons. *Cell* **75**, 463-476.

Habif, J. C., Xie, C., de Celis, C., Ukhanov, K., Green, W. W., Moretta, J. C., Zhang, L., Campbell, R. J. and Martens, J. R. (2023). The role of a ciliary GTPase in the regulation of neuronal maturation of olfactory sensory neurons. *Development* **150**.

Hanchate, N. K., Giacobini, P., Lhuillier, P., Parkash, J., Espy, C., Fouveaut, C., Leroy, C., Baron, S., Campagne, C., Vanacker, C., et al. (2012). SEMA3A, a gene involved in axonal pathfinding, is mutated in patients with Kallmann syndrome. *PLoS genetics* **8**, e1002896.

Herbison, A. E. (2025). Evolution of the GnRH Neuron. In *Evolutionary and Comparative Neuroendocrinology* (ed. V. Grinevich & R. Oliveira), pp. 143-164. Cham: Springer Nature Switzerland.

Hilal, E. M., Chen, J. H. and Silverman, A. J. (1996). Joint migration of gonadotropin-releasing hormone (GnRH) and neuropeptide Y (NPY) neurons from olfactory placode to central nervous system. *J Neurobiol* **31**, 487-502.

Hills, M. H., Ma, L., Fang, A., Chiremba, T., Malloy, S., Scott, A. R., Perera, A. G. and Yu, C. R. (2024). Molecular, cellular, and developmental organization of the mouse vomeronasal organ at single cell resolution. *Elife* **13**.

576 **Hirata, T., Nakazawa, M., Yoshihara, S., Miyachi, H., Kitamura, K., Yoshihara, Y. and Hibi,**
577 **M.** (2006). Zinc-finger gene Fez in the olfactory sensory neurons regulates development
578 of the olfactory bulb non-cell-autonomously. *Development* **133**, 1433-1443.
579 **Ikeda, K., Ookawara, S., Sato, S., Ando, Z., Kageyama, R. and Kawakami, K.** (2007). Six1 is
580 essential for early neurogenesis in the development of olfactory epithelium. *Dev Biol*
581 **311**, 53-68.
582 **Jasoni, C. L., Porteous, R. W. and Herbison, A. E.** (2009). Anatomical location of mature
583 GnRH neurons corresponds with their birthdate in the developing mouse. *Dev Dyn* **238**,
584 524-531.
585 **Kallmann, F.** (1944). The genetic aspects of primary eunuchoidism.
586 **Kamiya, C., Ohta, N., Ogura, Y., Yoshida, K., Horie, T., Kusakabe, T. G., Satake, H. and**
587 **Sasakura, Y.** (2014). Nonreproductive role of gonadotropin-releasing hormone in the
588 control of ascidian metamorphosis. *Dev Dyn* **243**, 1524-1535.
589 **Kaneko-Goto, T., Sato, Y., Katada, S., Kinameri, E., Yoshihara, S., Nishiyori, A., Kimura, M.,**
590 **Fujita, H., Touhara, K., Reed, R. R., et al.** (2013). Goofy coordinates the acuity of
591 olfactory signaling. *J Neurosci* **33**, 12987-12996, 12996a.
592 **Karns, L. R., Ng, S. C., Freeman, J. A. and Fishman, M. C.** (1987). Cloning of complementary
593 DNA for GAP-43, a neuronal growth-related protein. *Science* **236**, 597-600.
594 **Katoh, H., Shibata, S., Fukuda, K., Sato, M., Satoh, E., Nagoshi, N., Minematsu, T.,**
595 **Matsuzaki, Y., Akazawa, C., Toyama, Y., et al.** (2011). The dual origin of the peripheral
596 olfactory system: placode and neural crest. *Mol Brain* **4**, 34.
597 **Katreddi, R. R., Taroc, E. Z. M., Hicks, S. M., Lin, J. M., Liu, S. T., Xiang, M. Q. and Forni, P.**
598 **E.** (2022). Notch signaling determines cell-fate specification of the two main types of
599 vomeronasal neurons of rodents. *Development* **149**.
600 **Klein, S. L. and Graziadei, P. P.** (1983). The differentiation of the olfactory placode in Xenopus
601 laevis: a light and electron microscope study. *J Comp Neurol* **217**, 17-30.
602 **LeFever, N. M., Katreddi, R. R., Dolphin, N. M., Mathias, N. A. and Forni, P. E.** (2024).
603 Following the p63/Keratin5 basal cells in the sensory and non-sensory epithelia of the
604 vomeronasal organ. *Genesis* **62**, e23596.
605 **Lieblich, J. M., Rogol, A. D., White, B. J. and Rosen, S. W.** (1982). Syndrome of anosmia with
606 hypogonadotropic hypogonadism (Kallmann syndrome): clinical and laboratory studies in
607 23 cases. *Am J Med* **73**, 506-519.
608 **Lin, J. M., Mitchell, T. A., Rothstein, M., Pehl, A., Taroc, E. Z. M., Katreddi, R. R., Parra, K.**
609 **E., Zuloaga, D. G., Simoes-Costa, M. and Forni, P. E.** (2022). Sociosexual behavior
610 requires both activating and repressive roles of Tfap2e/AP-2epsilon in vomeronasal
611 sensory neurons. *Elife* **11**.
612 **Lin, J. M., Taroc, E. Z. M., Frias, J. A., Prasad, A., Catizone, A. N., Sammons, M. A. and**
613 **Forni, P. E.** (2018). The transcription factor Tfap2e/AP-2epsilon plays a pivotal role in
614 maintaining the identity of basal vomeronasal sensory neurons. *Dev Biol* **441**, 67-82.
615 **Lund, C., Yellapragada, V., Vuoristo, S., Balboa, D., Trova, S., Allet, C., Eskici, N., Pulli, K.,**
616 **Giacobini, P., Tuuri, T., et al.** (2020). Characterization of the human GnRH neuron
617 developmental transcriptome using a GNRH1-TdTomato reporter line in human
618 pluripotent stem cells. *Dis Model Mech* **13**.
619 **Margolis, F. L.** (1972). A brain protein unique to the olfactory bulb. *Proc Natl Acad Sci U S A* **69**,
620 1221-1224.
621 **Margolis, F. L. and Tarnoff, J. F.** (1973). Site of biosynthesis of the mouse brain olfactory bulb
622 protein. *J Biol Chem* **248**, 451-455.
623 **Miller, A. M., Treloar, H. B. and Greer, C. A.** (2010). Composition of the migratory mass during
624 development of the olfactory nerve. *J Comp Neurol* **518**, 4825-4841.

Murakami, S., Ohki-Hamazaki, H. and Uchiyama, Y. (2022). Olfactory placode generates a diverse population of neurons expressing GnRH, somatostatin mRNA, neuropeptide Y, or calbindin in the chick forebrain. *J Comp Neurol* **530**, 2977-2993.

---- (2024). Somatostatin affects GnRH neuronal development and migration and stimulates olfactory-related fiber fasciculation. *Dev Neurobiol* **84**, 3-17.

Paronett, E. M., Bryan, C. A., Maynard, T. M. and LaMantia, A.-S. (2023). Identity, lineage and fates of a temporally distinct progenitor population in the embryonic olfactory epithelium. *Developmental Biology*.

Poncelet, G. and Shimeld, S. M. (2020). The evolutionary origins of the vertebrate olfactory system. *Open Biol* **10**, 200330.

Rawson, N. E. (1999). Cell and molecular biology of olfaction. *Quintessence Int* **30**, 335-341.

Rawson, N. E., Lischka, F. W., Yee, K. K., Peters, A. Z., Tucker, E. S., Meechan, D. W., Zirlinger, M., Maynard, T. M., Burd, G. B., Dulac, C., et al. (2010). Specific mesenchymal/epithelial induction of olfactory receptor, vomeronasal, and gonadotropin-releasing hormone (GnRH) neurons. *Dev Dyn* **239**, 1723-1738.

Rukh, S., Meechan, D. W., Maynard, T. M. and Lamantia, A. S. (2024). Out of Line or Altered States? Neural Progenitors as a Target in a Polygenic Neurodevelopmental Disorder. *Dev Neurosci* **46**, 1-21.

Sakai, T., Yamamoto, T., Matsubara, S., Kawada, T. and Satake, H. (2020). Invertebrate Gonadotropin-Releasing Hormone Receptor Signaling and Its Relevant Biological Actions. *Int J Mol Sci* **21**.

Schwanzel-Fukuda, M. and Pfaff, D. W. (1989). Origin of luteinizing hormone-releasing hormone neurons. *Nature* **338**, 161-164.

Schwarting, G. A., Kostek, C., Bless, E. P., Ahmad, N. and Tobet, S. A. (2001). Deleted in colorectal cancer (DCC) regulates the migration of luteinizing hormone-releasing hormone neurons to the basal forebrain. *J Neurosci* **21**, 911-919.

Shan, Y., Saadi, H. and Wray, S. (2020). Heterogeneous Origin of Gonadotropin Releasing Hormone-1 Neurons in Mouse Embryos Detected by Islet-1/2 Expression. *Front Cell Dev Biol* **8**, 35.

Smart, I. H. (1971). Location and orientation of mitotic figures in the developing mouse olfactory epithelium. *J Anat* **109**, 243-251.

Stolfi, A., Ryan, K., Meinertzhagen, I. A. and Christiaen, L. (2015). Migratory neuronal progenitors arise from the neural plate borders in tunicates. *Nature* **527**, 371-374.

Taroc, E. Z. M., Lin, J. M., Tulloch, A. J., Jaworski, A. and Forni, P. E. (2019). GnRH-1 Neural Migration From the Nose to the Brain Is Independent From Slit2, Robo3 and NELL2 Signaling. *Front Cell Neurosci* **13**, 70.

Taroc, E. Z. M., Naik, A. S., Lin, J. M., Peterson, N. B., Keefe, D. L., Jr., Genis, E., Fuchs, G., Balasubramanian, R. and Forni, P. E. (2020). Gli3 Regulates Vomeronasal Neurogenesis, Olfactory Ensheathing Cell Formation, and GnRH-1 Neuronal Migration. *J Neurosci* **40**, 311-326.

Taroc, E. Z. M., Prasad, A., Lin, J. M. and Forni, P. E. (2017). The terminal nerve plays a prominent role in GnRH-1 neuronal migration independent from proper olfactory and vomeronasal connections to the olfactory bulbs. *Biol Open* **6**, 1552-1568.

Tarozzo, G., Peretto, P. and Fasolo, A. (1995). Cell migration from the olfactory placode and the ontogeny of the neuroendocrine compartments. *Zoolog Sci* **12**, 367-383.

Umatani, C. and Oka, Y. (2019). Multiple functions of non-hypophysiotropic gonadotropin releasing hormone neurons in vertebrates. *Zoological Lett* **5**, 23.

Valverde, F., Heredia, M. and Santacana, M. (1993). Characterization of neuronal cell varieties migrating from the olfactory epithelium during prenatal development in the rat. Immunocytochemical study using antibodies against olfactory marker protein (OMP) and luteinizing hormone-releasing hormone (LH-RH). *Brain Res Dev Brain Res* **71**, 209-220.

Verhaagen, J., Oestreicher, A. B., Gispen, W. H. and Margolis, F. L. (1989). The expression of the growth associated protein B50/GAP43 in the olfactory system of neonatal and adult rats. *J Neurosci* **9**, 683-691.

Verwoerd, C. D. and van Oostrom, C. G. (1979). Cephalic neural crest and placodes. *Adv Anat Embryol Cell Biol* **58**, 1-75.

Vilensky, J. A. (2012). The neglected cranial nerve: Nervus terminalis (cranial nerve N). *Clin Anat*.

Whitlock, K. E. and Westerfield, M. (2000). The olfactory placodes of the zebrafish form by convergence of cellular fields at the edge of the neural plate. *Development* **127**, 3645-3653.

Wierman, M. E., Kiseljak-Vassiliades, K. and Tobet, S. (2011). Gonadotropin-releasing hormone (GnRH) neuron migration: initiation, maintenance and cessation as critical steps to ensure normal reproductive function. *Front Neuroendocrinol* **32**, 43-52.

Wray, S., Grant, P. and Gainer, H. (1989). Evidence that cells expressing luteinizing hormone-releasing hormone mRNA in the mouse are derived from progenitor cells in the olfactory placode. *P Natl Acad Sci USA* **86**, 8132-8136.

Wray, S., Key, S., Qualls, R. and Fueshko, S. M. (1994). A subset of peripherin positive olfactory axons delineates the luteinizing hormone releasing hormone neuronal migratory pathway in developing mouse. *Dev Biol* **166**, 349-354.

Yoshida, K., Tobet, S. A., Crandall, J. E., Jimenez, T. P. and Schwarting, G. A. (1995). The migration of luteinizing hormone-releasing hormone neurons in the developing rat is associated with a transient, caudal projection of the vomeronasal nerve. *J Neurosci* **15**, 7769-7777.

Zouaghi, Y., Alpern, D., Gardeux, V., Russeil, J., Deplancke, B., Santoni, F., Pitteloud, N. and Messina, A. (2025). Transcriptomic profiling of murine GnRH neurons reveals developmental trajectories linked to human reproduction and infertility. *Theranostics* **15**, 3673-3692.

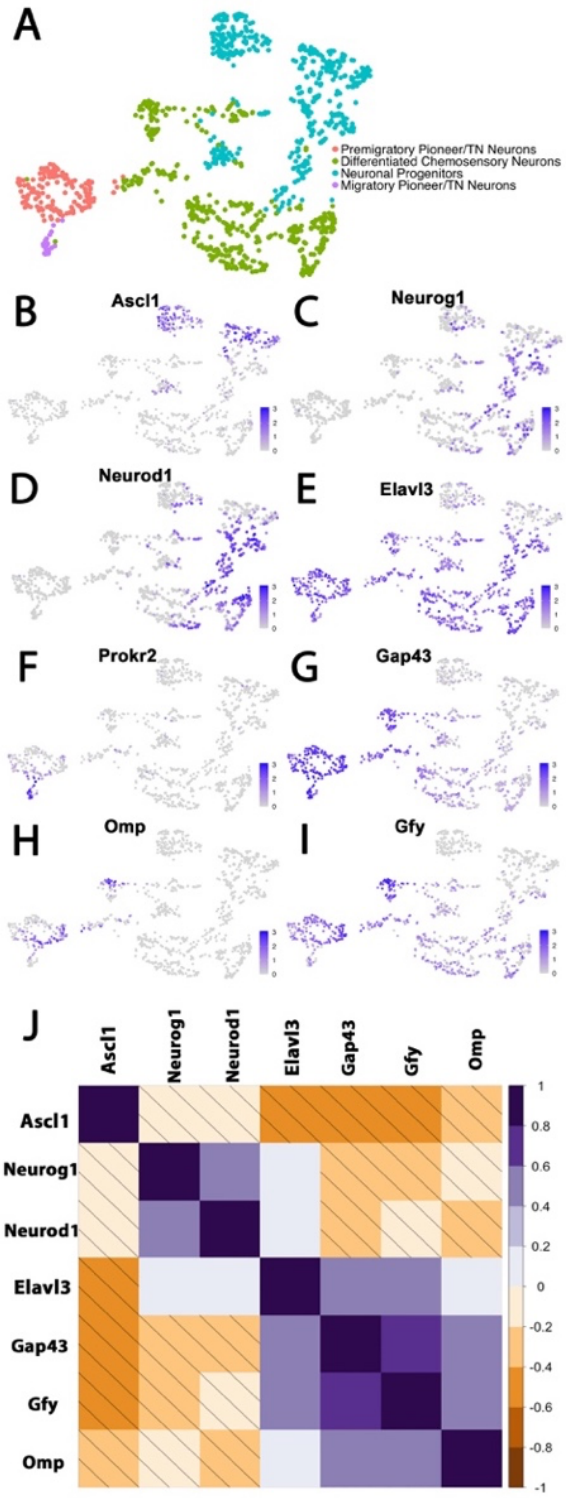

Figure 1. Gfy expression in the developing olfactory system. A) UMAP of neuronal populations in the developing olfactory system at E14.5 generated from single-cell RNA sequencing of the nasal area. B–I) Feature plots showing expression of for Ascl1, Neurog1, Neurod1, Elav3, Prokr2, Gap43, Omp, and Gfy. Progenitor markers (Ascl1, Neurog1) precede neuronal differentiation markers (Neurod1, Elavl3), while Gap43 labels immature neurons and Omp marks mature sensory neurons. Gfy is enriched in differentiating and

immature neuronal populations. J) Correlation matrix showing negative correlations (diagonal lines) between progenitor and maturation markers and positive correlations between Gfy and neuronal differentiation genes.

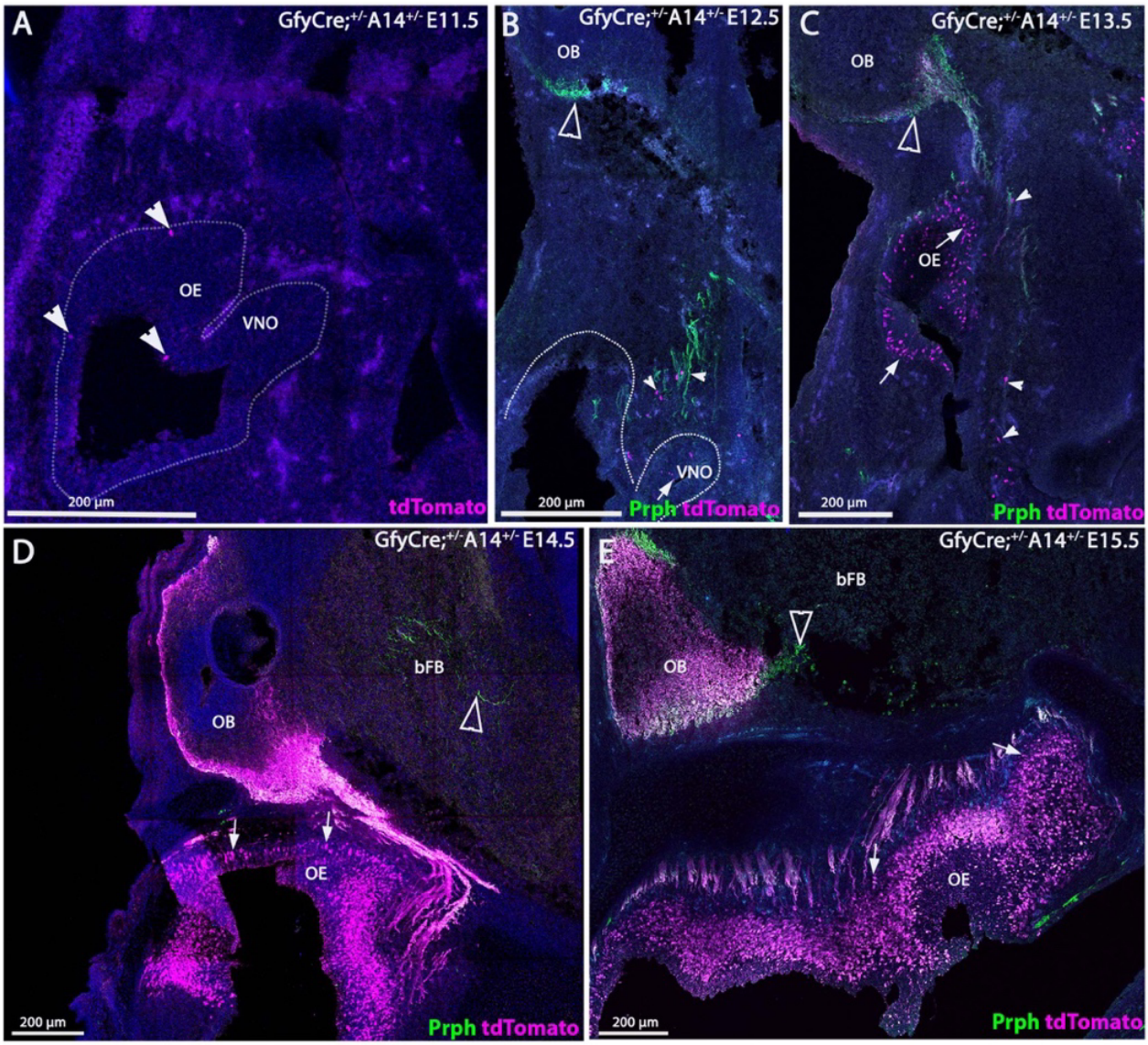

Figure 2. Time course of Gfy genetic lineage tracing in the developing olfactory system. A) At E11.5, GfyCre$^{+/-}$;Ai14$^{+/-}$ parasagittal sections show sparse Gfy lineage tracing (magenta) in the olfactory epithelium (OE) and vomeronasal organ (VNO). B) At E12.5, Gfy tracing is detected in both chemosensory neurons (tailed arrows) and migratory neurons (white notched arrowheads), closely associated with peripherin-positive fibers (Prph, green), including near the olfactory bulb (OB). C) At E13.5, Gfy-traced cells are present in the OE (tailed arrows) and within the peripherin-positive migratory mass (notched arrowheads); peripherin-positive axons positive for the tracing are visible near the OB (open arrowhead).

D–E) At E14.5 and E15.5, Gfy tracing becomes abundant throughout the nasal epithelium, particularly in the OE (tailed arrows). In contrast, Peripherin-positive axons projecting to the basal forebrain and peripherin positive migratory neurons in the basal forebrain (bFB) are largely Gfy-negative (open arrowheads). Scale bars, 200 µm.

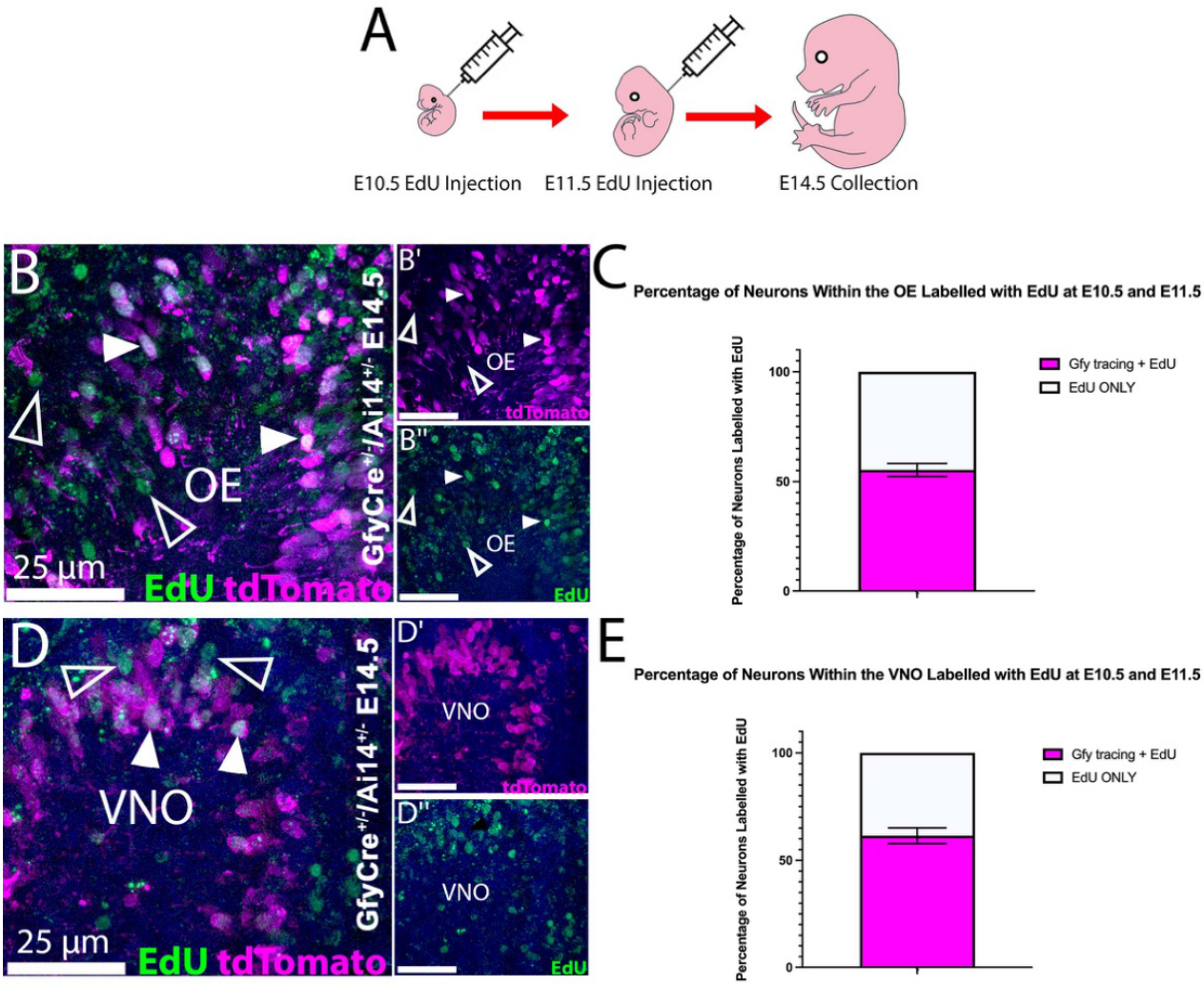

Figure 3. Gfy lineage tracing labels early-born chemosensory neurons.
A) Schematic of EdU birth-dating experiments: EdU injections at E10.5 and E11.5 followed by tissue collection at E14.5. B–B") GfyCre+/−;Ai14+/− E14.5 olfactory epithelium (OE) sections stained for EdU (green) and Gfy lineage tracing (tdTomato, magenta). Gfy-traced neurons (open arrowheads) include a substantial fraction that is EdU-positive (filled arrowheads). C) Quantification of EdU-positive neurons in the OE showing the proportion that is Gfy-traced versus EdU-only. D–D") GfyCre+/−;Ai14+/− E14.5 vomeronasal organ (VNO) sections stained for EdU and Gfy tracing. E) Quantification of EdU-positive neurons in the VNO showing the proportion that is Gfy-traced versus EdU-only. Scale bars, 25 µm.

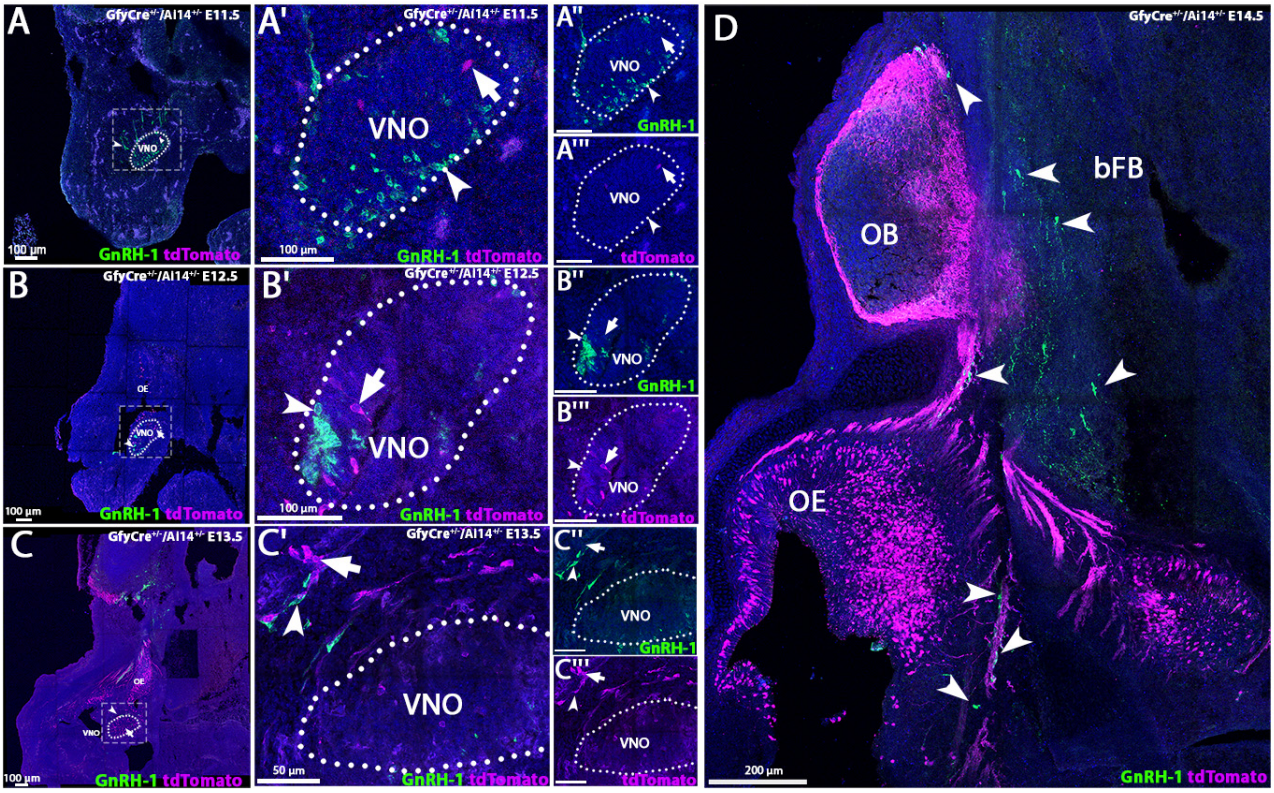

Figure 4. GnRH-1 neurons do not express Gfy.
Parasagittal sections from GfyCre$^{+/-}$;Ai14$^{+/-}$ embryos at E11.5-E14.5 stained for GnRH-1 (green)(arrowheads). A-A‴) At E11.5, GnRH-1 neurons are located within and emerging from the vomeronasal organ (VNO), while Gfy lineage tracing (magenta) is sparse (arrows). B-B‴) At E12.5, Gfy-traced neurons increase in the VNO and olfactory epithelium (OE), coinciding with continued GnRH-1 neuronal migration. C-C‴) By E13.5, GnRH-1 neurons begin invading the brain, whereas Gfy tracing remains restricted to the nasal compartment. D) At E14.5, GnRH-1 neurons reach the basal forebrain (bFB); Gfy tracing is abundant in the nasal epithelium and detectable in the olfactory bulb (OB) but remains absent from GnRH-1 neurons. Scale bars: D, 200 µm; A-C and A'-B‴, 100 µm; C'-C‴, 50 µm.

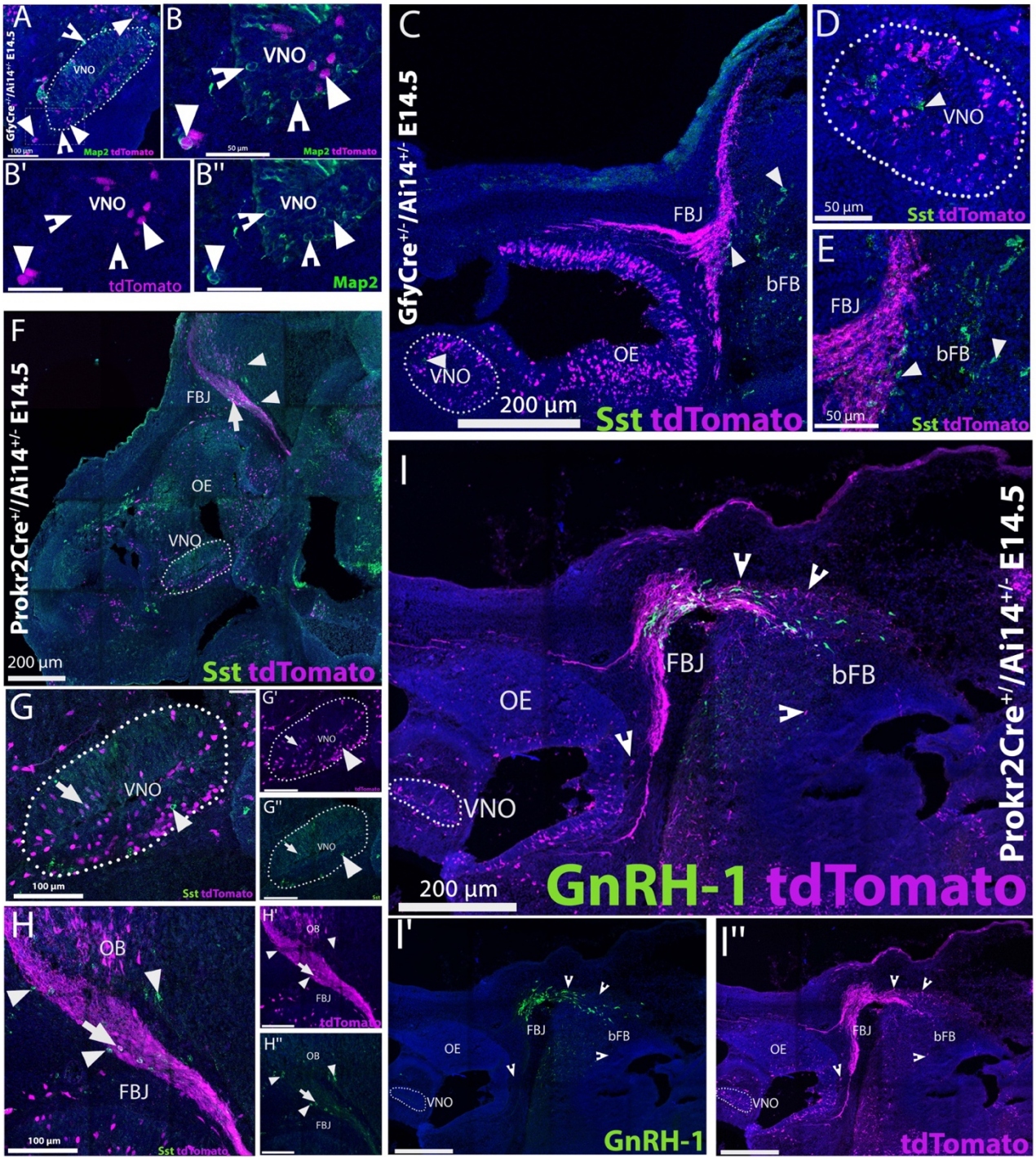

Figure 5. A subpopulation of the migratory mass neurons express Gfy, but do not invade the brain.

A-B'') GfyCre$^{+/-}$/Ai14$^{+/-}$ embryos at E13.5 paired with TN marker Map2 (green) immunofluorescent staining (notched arrows). Many Map2+ TN neurons were observed to migrate in clusters out of the vomeronasal organ (VNO). Gfy traced neurons (magenta)

806 were observed in the VNO, and olfactory epithelium (OE) and migratory mass. Many of the
807 migratory Gfy traced neurons appeared to be Map2+ (arrows). C-E) E14.5 GfyCre$^{+/-}$/Ai14$^{+/-}$
808 embryos stained for Somatostatin (Sst, green). Sst neurons in the migratory mass near the
809 forebrain junction (FBJ) and basal forebrain (bFB) are not positive for Gfy tracing
810 (arrowheads). F-H'') Prokr2Cre$^{+/-}$/Ai14$^{+/-}$ E14.5 sections stained with Sst. Prokr2 tracing
811 appears to overlap with Sst expression in both the VNO and migratory mass near the FBJ. I-
812 I'') Prokr2Cre$^{+/-}$/Ai14$^{+/-}$ E14.5 embryos paired with GnRH-1 immunofluorescent staining.
813 Prokr2 traced cell bodies and fibers migrate from the nose (notched arrowheads) invade
814 the brain, distinct from the GnRH-1 neurons. Scale bars in C,F,I-I'', 200 μm; A, G-G'', H-H'',
815 100 μm; B-B'', D,E, G-G'', 50 μm.

816

817

818

819

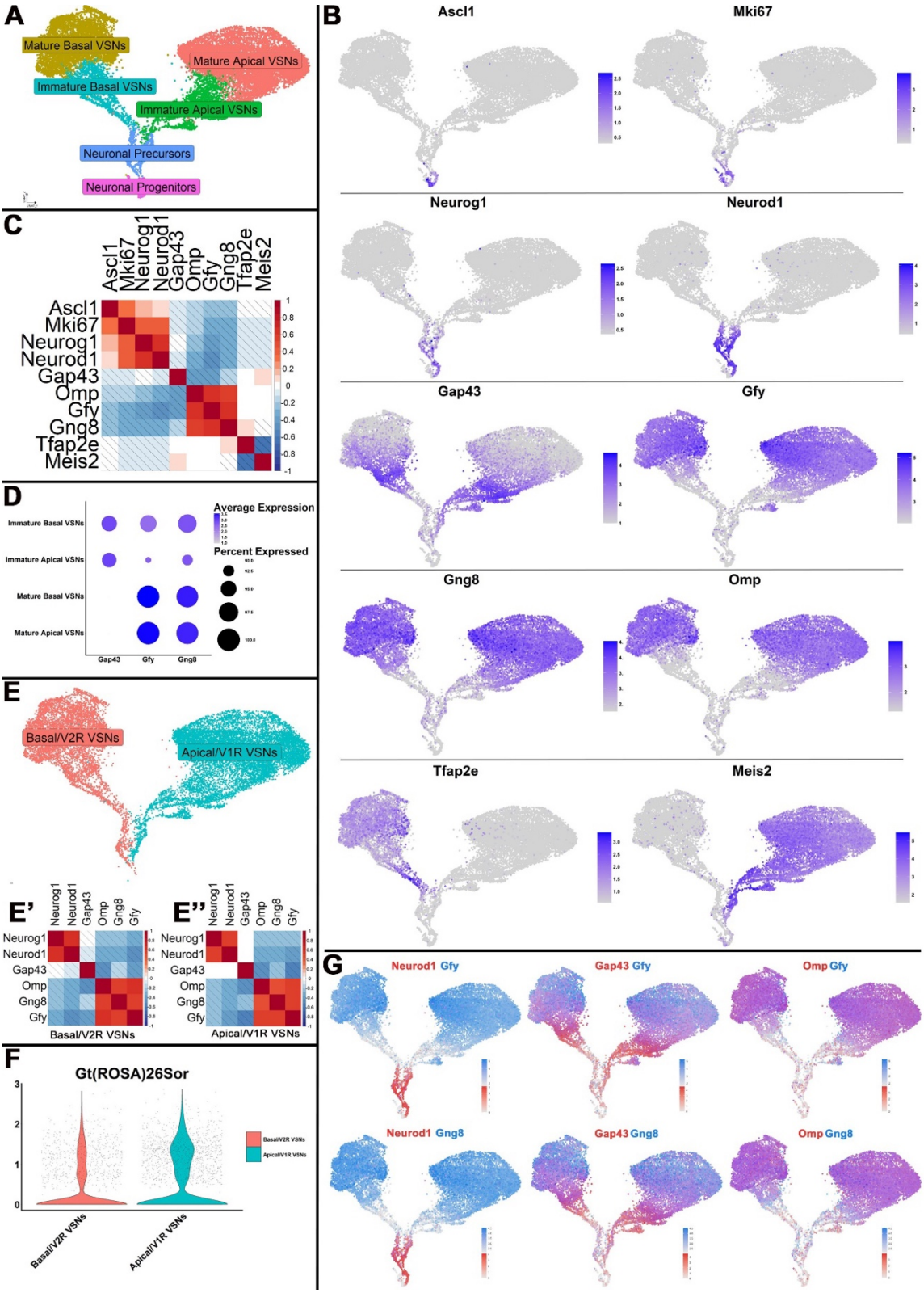
A
Mature Basal VSNs
Mature Apical VSNs
Immature Basal VSNs
Immature Apical VSNs
Neuronal Precursors
Neuronal Progenitors
B
Ascl1
Mki67
Neurog1
Neurod1
Gap43
Gfy
Gng8
Omp
Tfap2e
Meis2
C
Ascl1
Mki67
Neurog1
Neurod1
Gap43
Omp
Gfy
Gng8
Tfap2e
Meis2
D
Immature Basal VSNs
Immature Apical VSNs
Mature Basal VSNs
Mature Apical VSNs
Gap43
Gfy
Gng8
Average Expression
Percent Expressed
E
Basal/V2R VSNs
Apical/V1R VSNs
E'
E''
Neurog1
Neurod1
Gap43
Omp
Gng8
Gfy
Basal/V2R VSNs
Apical/V1R VSNs
F
Gt(ROSA)26Sor
Basal/V2R VSNs
Apical/V1R VSNs
G
Neurod1 Gfy
Gap43 Gfy
Omp Gfy
Neurod1 Gng8
Gap43 Gng8
Omp Gng8

Figure 6. Single-cell transcriptomic analysis of the postnatal vomeronasal organ. A) UMAP projection of scRNA-seq data from the postnatal vomeronasal organ illustrating the major neuronal populations, including Neuronal Progenitors, Neuronal Precursors, Immature apical and basal VSNs, and mature V1R/Meis2+ and V2R/AP-2ε+ VSNs. The characteristic Y-shaped dichotomy of apical and basal lineages is resolved. B) UMAP feature plots showing expression of key developmental markers across the dataset. Ascl1 and Mki67 label proliferative progenitors, Neurog1 and Neurod1 label neuronal precursors, Gap43 marks immature neurons of both lineages, whereas Omp labels mature VSNs. Gfy and Gng8 are associated with early postmitotic neuronal states. Tfap2e and Meis2 highlight the basal and apical lineages, respectively. C) Correlation matrix illustrating co-expression patterns among canonical developmental and lineage-specific markers. Strong positive correlations identify the sequential transitions from progenitors to neuronal precursors to immature and mature VSNs. Negative correlations indicated with diagonal lines. D) Dot plot summarizing Gap43, Gfy, and Gng8 expression across immature and mature apical and basal VSNs. Average expression and percent of expressing cells show that Gfy and Gng8 are lowly expressed in immature stages and are enriched upon maturation. E) UMAP projections showing the apical (V1R/Meis2+) and basal (V2R/Tfap2e+) VSN lineages segregated for comparison. E'–E") Correlation matrices demonstrating that the developmental progression of apical and basal VSNs involves similar transcriptional transitions, but with distinct lineage-specific marker relationships. F) Violin plots comparing expression of the Gt(ROSA)26Sor locus between basal and apical VSNs, revealing differential baseline activity of the ROSA locus across lineages. (G) Co-expression UMAPs illustrating the spatial and developmental relationships of Gfy and Gng8 with Neurod1, Gap43, and Omp, highlighting that Gfy and Gng8 mark neurons before and after they reach full maturation.

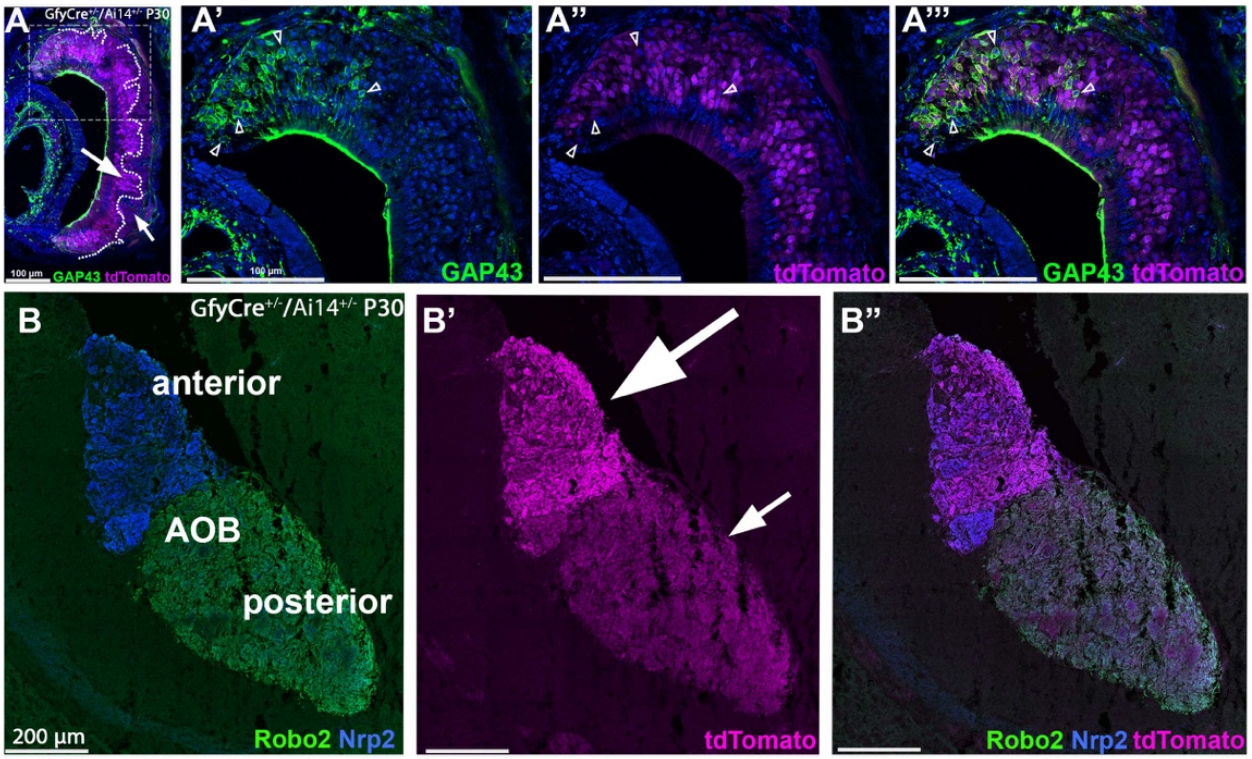

Figure 7. GfyCre-traced neurons in the VNO and AOB exhibit distinct levels of Gfy expression. A) Postnatal day 30 (P30) GfyCre$^{+/-}$;Ai14$^{+/-}$ vomeronasal organ (VNO) coronal sections stained for the immature vomeronasal sensory neuron (VSN) marker Gap43 (green) and tdTomato (red). Gfy lineage tracing (magenta) is detected at lower levels in neurons in the basal territories (small arrows) and at higher levels in VSNs in the apical regions (larger arrows). A'-A''' enlargements of the marginal zone (boxed in (A)) showing GAP43; tdTomato and merge A'''). Arrows indicate GAP43 immunoreactive cells negative for tdTomato or expressing below detectability. B–B") P30 GfyCre$^{+/-}$;Ai14$^{+/-}$ accessory olfactory bulb (AOB) sections stained for Robo2 (green) and Nrp2 (blue) to distinguish posterior and anterior AOB projections, respectively. B'-B") GfyCre tracing (magenta) is present in both anterior and posterior AOB regions but appears weaker in the Nrp2-positive posterior AOB (small arrows) compared with the anterior AOB (large arrows). Scale bars: A–A''', 100 µm; B–B", 200 µm.

Supplementary Figures

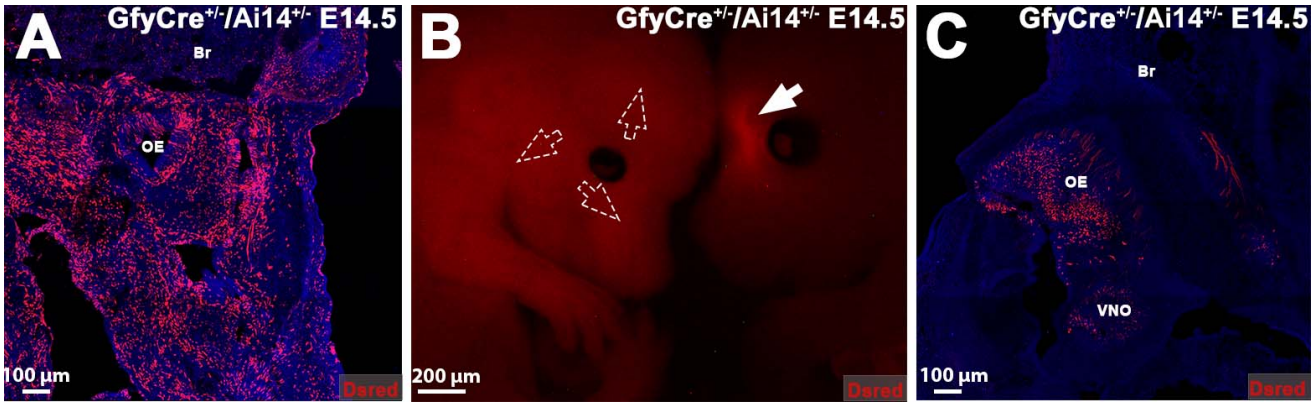

Figure S1.
GfyCre Non-specific Recombination.
A) An E14.5 GfyCre$^{+/-}$/Ai14$^{+/-}$ with nonspecific, broad chimeric tracing throughout the nasal area including the olfactory epithelium (OE). B) Whole-embryo imaging comparing a GfyCre$^{+/-}$/Ai14$^{+/-}$ embryo with nonspecific tracing present throughout the whole body (left) and a GfyCre$^{+/-}$/Ai14$^{+/-}$ embryo with correct tracing exclusive to the olfactory system (right, arrow). C) A correctly traced GfyCre$^{+/-}$/Ai14$^{+/-}$ E14.5 embryo, Gfy tracing can be visualized in the developing vomeronasal organ (VNO) and OE. Scale bars in B, 200 µm; A,C, 100 µm.

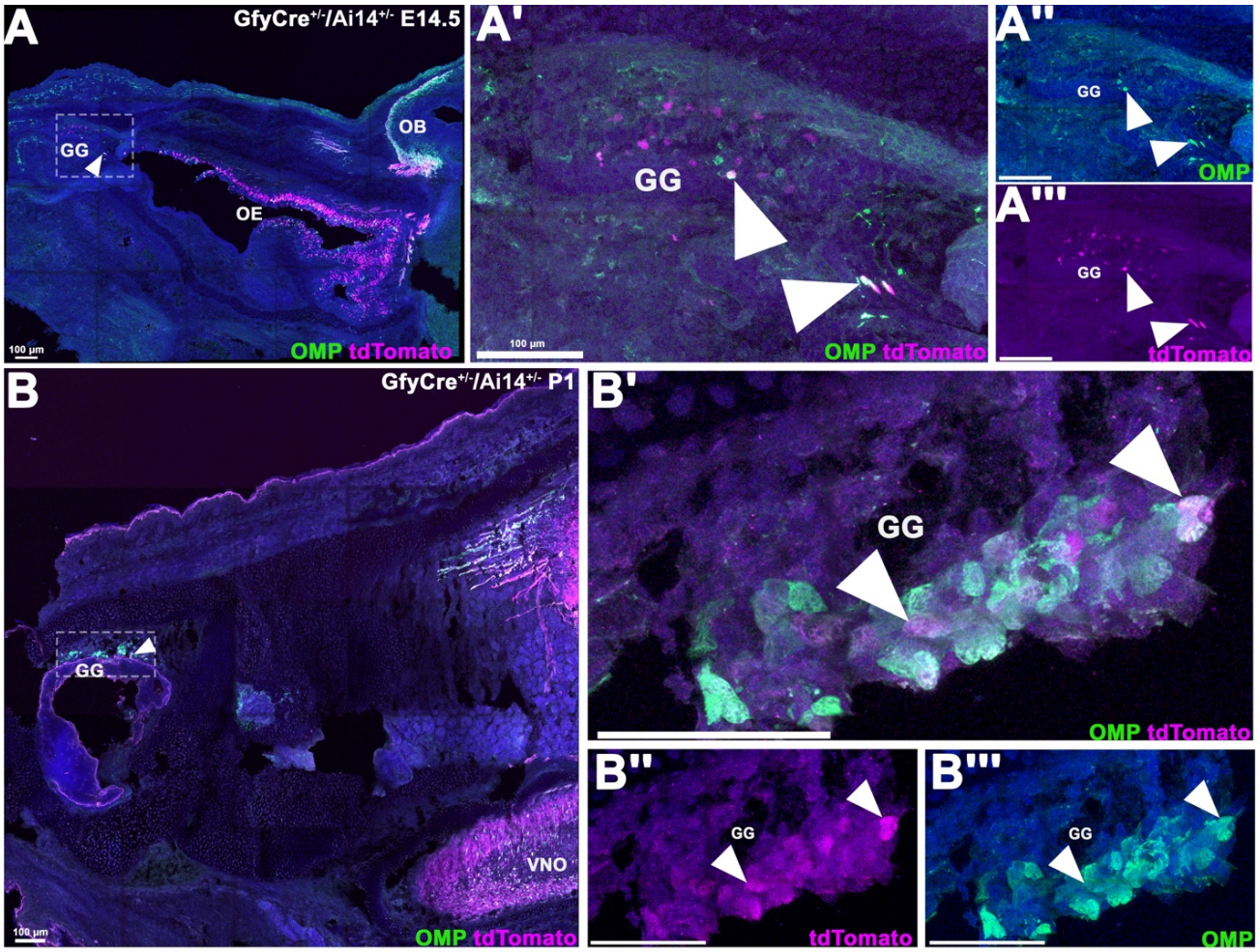

Figure S2.

The Grueneberg Ganglion Expresses Gfy.

A-A''') E14.5 GfyCre$^{+/-}$/Ai14$^{+/-}$ embryos immunostained for Omp (green). Gfy tracing can be observed in the olfactory bulb (OB), olfactory epithelium (OE) and the neurons of the Grueneberg ganglion (GG) (arrowheads). B-B''') P2 GfyCre$^{+/-}$/Ai14$^{+/-}$ animals show increased Gfy tracing in the vomeronasal organ (VNO) and GG. Scale bars in A-B''', D, 100 µm.

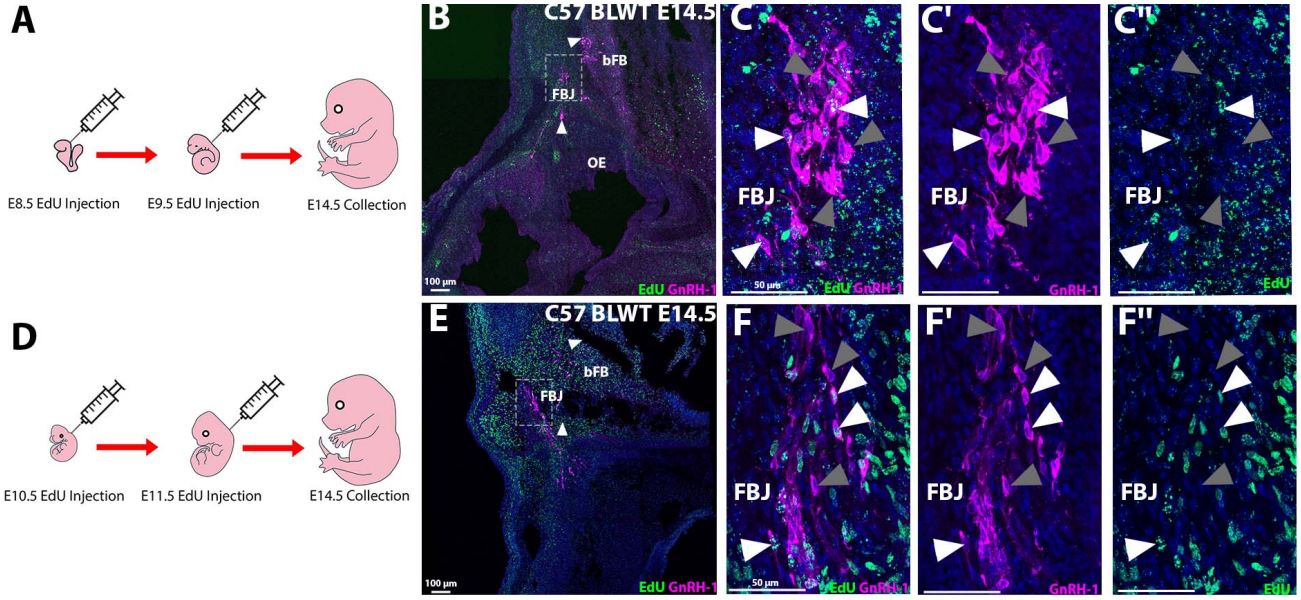

Figure S3.

GnRH-1 EdU Birth-dating Experiments.

A) Schematic of E8.5 and E9.5 EdU injection experiments, then collection at E14.5. B-C'') E14.5 C57 BLWT control tissue immunostained for EdU (green) and GnRH-1 (magenta, grey arrowheads). D) Schematic of E10.5 and E11.5 EdU injection experiments, then collection at E14.5. E-F'') EdU labelling at E10.5 and E11.5 was abundant in the forebrain junction (FBJ) and basal forebrain (bFB), overlapping with GnRH-1 immunoreactivity (white arrowheads). Scale bars in B, E 100 µm; C-C'', F-F'', 50 µm.

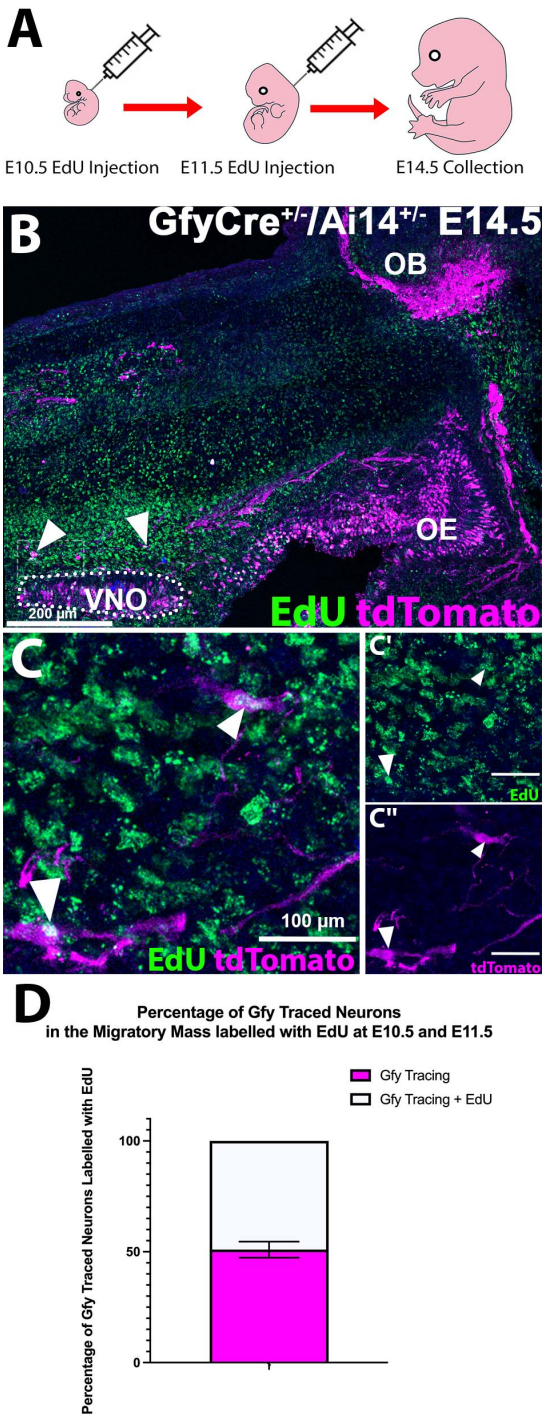

Figure S4.

Gfy Tracing EdU Brith-dating Experiments in Migratory Mass.

A) Schematic of EdU injection experiments performed at E10.5 and E11.5 and subsequently collected at E14.5. B) Parasagittal section on E14.5 GfyCre$^{+/-}$ /Ai14$^{+/-}$ embryos stained for EdU (green) and Gfy tracing (magenta). C-C'') Gfy tracing (magenta) and EdU staining (green) overlap (white) indicated with the arrowheads. D) Quantifications of EdU positive Gfy traced migratory neurons in the migratory mass. Scale bars in B, 200 µm; C-C'', 100 µm.

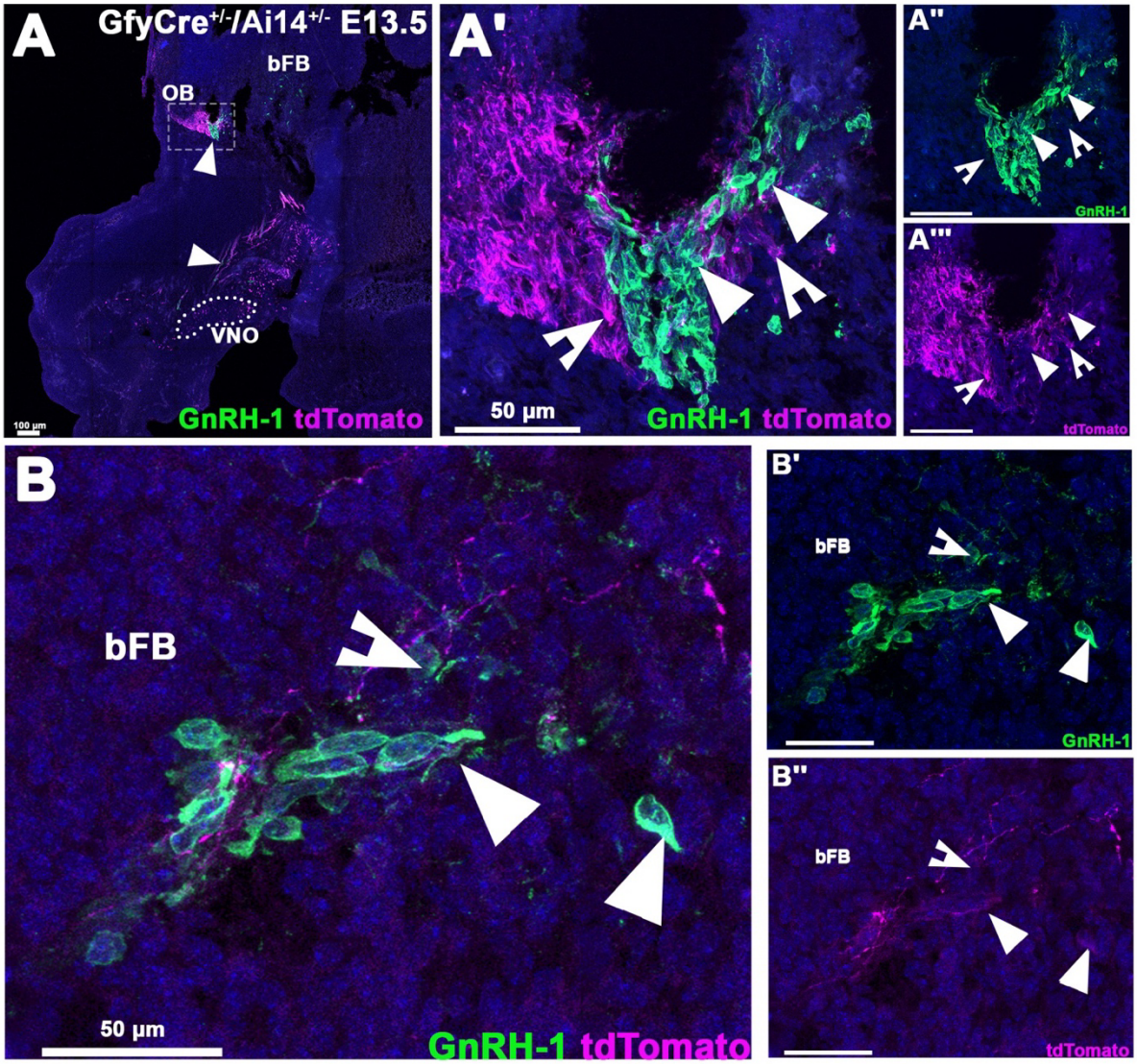

Figure S5.

The GnRH-1 neurons are closely intertwined with Gfy traced fibers in the brain.

A-A'') E13.5 GfyCre$^{+/-}$/Ai14$^{+/-}$ sections paired with GnRH-1 immunofluorescent staining. At this stage, GnRH-1 neurons (green, arrowheads) are migrating out of the vomeronasal organ (VNO), surrounded by Gfy traced cell bodies and axons/fibers (magenta, notched arrowheads) that also appear to be migrating out of the VNO. The GnRH-1 neurons invading the brain are not traced for Gfy. B-B'') GnRH-1 neurons invading the basal forebrain (bFB) with faint Gfy traced fibers entangling the GnRH-1 neurons and some Gfy traced cell bodies entering the brain. Scale bars in A, 100 µm; B-B'', C-C'', 50 µm.

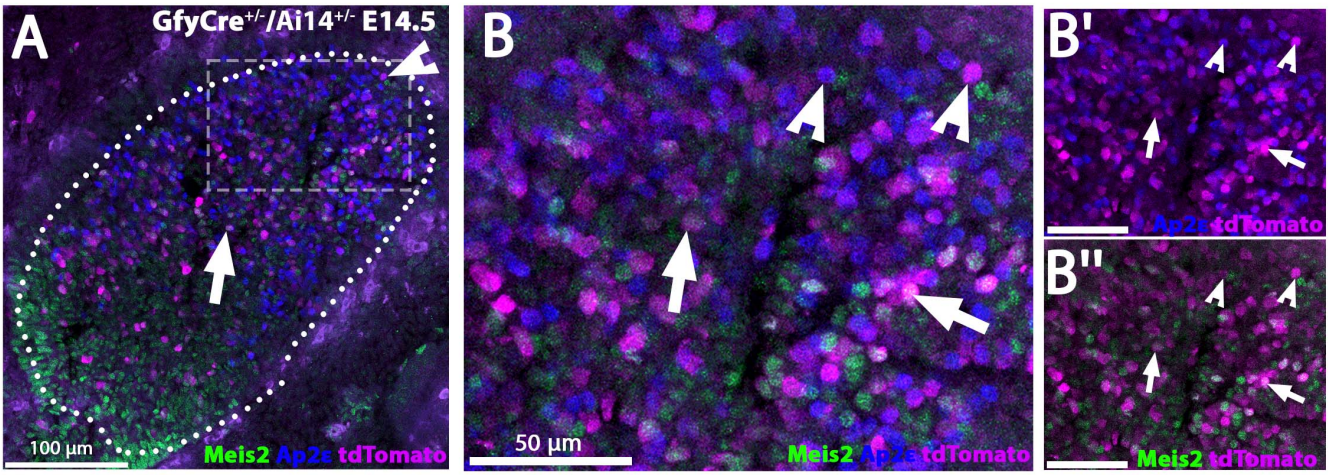

Figure S6. Genetic lineage tracing of Gfy in the embryonic VNO.
A-B'') E14.5 GfyCre$^{+/-}$/Ai14$^{+/-}$ vomeronasal organ (VNO) sections stained for vomeronasal sensory neuron (VSN) populations, Meis2 (green, arrows, apical) and AP-2ε (blue, notched arrowheads, basal). Both apical and basal developing VSNs were positive for Gfy tracing at E14.5. Scale bars in A, 100 µm; B-B'', 50 µm.

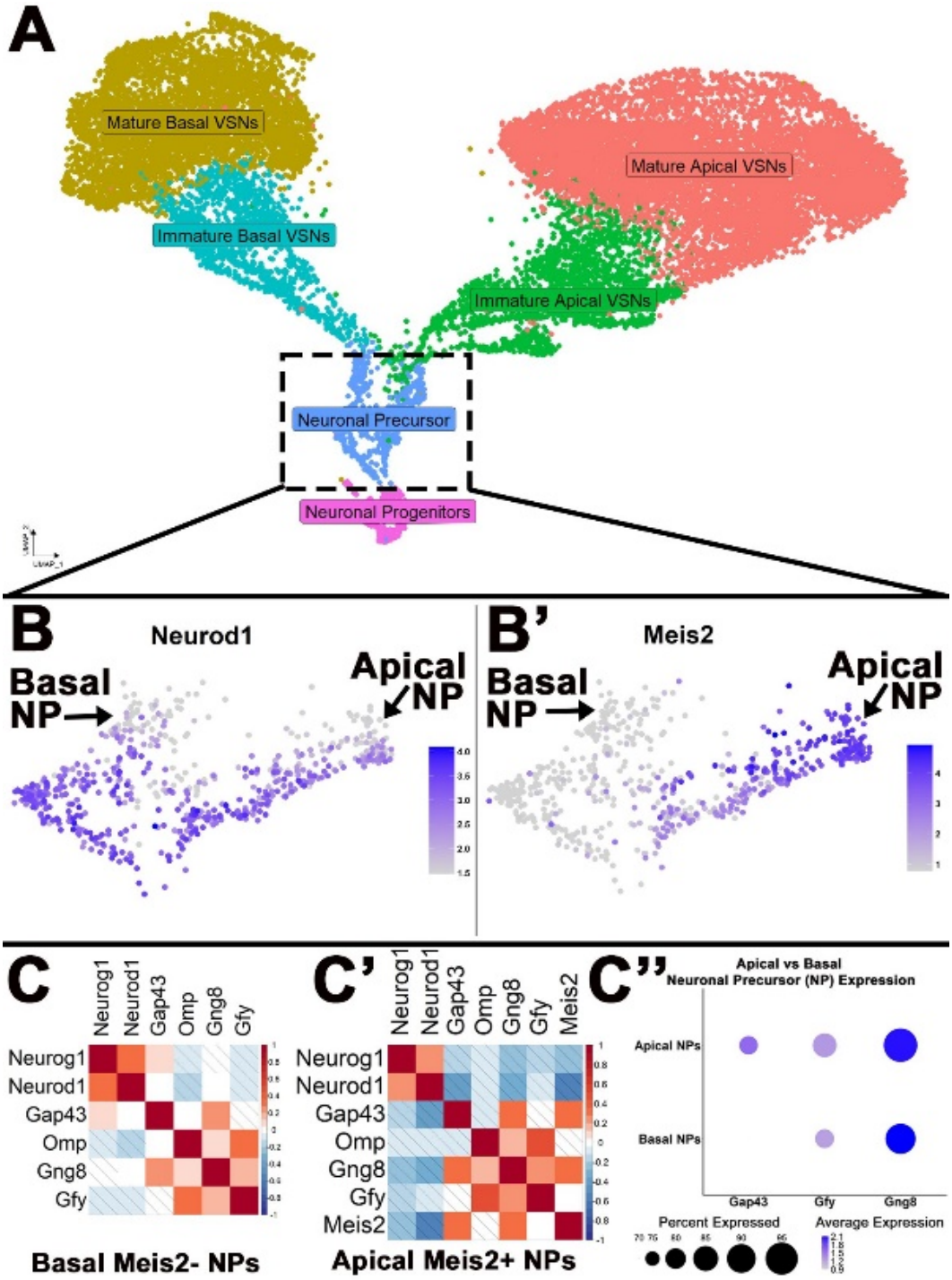
A
Mature Basal VSNs
Mature Apical VSNs
Immature Basal VSNs
Immature Apical VSNs
Neuronal Precursor
Neuronal Progenitors
B
Neurod1
Basal NP
Apical NP
B'
Meis2
Basal NP
Apical NP
C
Neurog1
Neurod1
Gap43
Omp
Gng8
Gfy
Basal Meis2- NPs
C'
Neurog1
Neurod1
Gap43
Omp
Gng8
Gfy
Meis2
Apical Meis2+ NPs
C''
Apical vs Basal
Neuronal Precursor (NP) Expression
Apical NPs
Basal NPs
Gap43
Gfy
Gng8
Percent Expressed
Average Expression

Figure S7. Single-cell transcriptomic analysis of the postnatal vomeronasal organ neuronal precursor populations.

A) UMAP projection of scRNA-seq data from the postnatal vomeronasal organ illustrating the major neuronal populations: the Neuronal Progenitors, Neuronal Precursors, immature apical and basal VSNs, and mature V1R/Meis2+ and V2R/AP-2ε+ VSNs. B-B') UMAP feature plots of the neuronal precursor population, Neurod1 highlights both apical and basal neuronal precursors (NP), while Meis2 expression is more enriched in apical neuronal precursors. C-C') Correlation matrix showing correlations between the neuronal precursor markers Neurod1 and key maturation markers (Gap43, Gng8, Gfy, Meis2). C'') Dotplot illustrating the expression pattern of Gap43, Gfy and Gng8 across both the apical basal populations of neuronal precursors.